

# **Research Article**

# Introduction to the *Thomasomys* (Rodentia: Cricetidae) turbinal adaptations: insights into elevational and environmental challenges

Dennisse Ruelas<sup>1,2,3,\*,10</sup>, Pierre-Henri Fabre<sup>3,4,5,10</sup>, Víctor Pacheco<sup>1,10</sup>, Quentin Martinez<sup>3,6,10</sup>

Associate Editor: Alexandre Percequillo

#### **Abstract**

Turbinal bones in mammals, due to their roles in thermoregulation and olfaction, are effective indicators for studying ecological habits. Hypothetically, larger respiratory turbinals aid in heat and moisture retention, particularly in challenging environments like those at high elevations. The Andes, with its diverse landscapes and high biodiversity, provides an ideal environment for such studies. Among Andean endemics, the genus Thomasomys—mostly restricted to montane forests and páramos—exhibits high species diversity and adaptability across elevational gradients, making it an ideal candidate for exploring the relationship between ecological niches, habitat selection, and turbinal morphology. Using 3D CT scans of Thomasomys turbinal bones, our study aims to understand the interplay between turbinal surface area and environmental factors (elevation and bioclimatic variables). Our findings reveal consistent turbinal morphological features among Thomasomys species, showing: (i) positive allometric relationships with skull length; (ii) an absence of evolutionary trade-offs between the nasoturbinals and maxilloturbinals and between respiratory and olfactory turbinals; (iii) influence of elevation on the turbinal surface area with lower-elevation species having comparatively smaller turbinal surface areas than higher-elevation species; and (iv) that bioclimatic variables show significant correlations with the proportion of respiratory and olfactory turbinals. Therefore, our results align with the general hypothesis that large respiratory turbinals may help in coping with harsh environmental conditions. However, the relation between elevation and olfactory turbinal surface areas remains puzzling. Various other ecological confounding factors appear to be present and are discussed. Overall, this study sheds light on the complex adaptations of turbinal bones and their interactions with environmental factors, contributing to our understanding of mammalian ecomorphology in montane forest habitats.

Key words: Andes, heat and moisture conservation, montane forest, olfaction, Sigmodontinae

Introducción a las adaptaciones de los huesos turbinados de Thomasomys (Rodentia: Cricetidae): perspectivas sobre la elevación y los desafíos ambientales

#### Resumen

Los huesos turbinados en mamíferos, debido a sus roles en la termorregulación y la olfacción, son indicadores efectivos en el estudio de los hábitos ecológicos. Hipotéticamente, huesos turbinados respiratorios más grandes ayudan a retener calor y humedad, especialmente en entornos desafiantes como aquellos en elevaciones altas. Los Andes, con sus paisajes diversos y alta biodiversidad, proporcionan un ambiente ideal para tales estudios. Entre las especies andinas endémicas, el género *Thomasomys*, principalmente restringido a bosques montanos y páramos, presenta una alta diversidad de especies y adaptabilidad a lo largo de varias gradientes altitudinales. Esto lo convierte en un candidato ideal para explorar la relación entre los nichos ecológicos, selección de hábitat y morfología de los huesos turbinados. Utilizando escaneos CT en 3D de los huesos turbinados de *Thomasomys*, nuestro análisis busca entender la interacción entre las adaptaciones de estos huesos y los factores ambientales (elevación y variables bioclimáticas). Nuestros hallazgos revelan que las características morfológicas de los huesos turbinados consistentes entre las especies de *Thomasomys*, mostrando (i) relaciones alométricas positivas con respecto a la longitud del cráneo, (ii) ausencia de una compensación evolutiva entre los huesos nasoturbinados y maxiloturbinados, e interesantemente, entre los huesos turbinados respiratorios y olfatorios; (iii) influencia de la elevación en el área de la superficie de estos huesos, donde las especies de menor elevación tienen áreas de superficie más pequeñas comparativamente, que aquellas especies de mayor elevación; y

<sup>&</sup>lt;sup>1</sup>Museo de Historia Natural, Universidad Nacional Mayor de San Marcos, Av. Arenales 1256, Lima 15072, Peru

<sup>&</sup>lt;sup>2</sup>Doctorado en Ciencias de la Vida, Universidad Peruana Cayetano Heredia, Av. Honorio Delgado 430, Lima 150135, Peru

Institut des Sciences de l'Évolution (ISEM, UMR 5554 CNRS-IRD-UM), Université de Montpellier, Place E. Bataillon—CC 064, Montpellier Cedex 5 34095, France

<sup>&</sup>lt;sup>4</sup>Mammal Section, Department of Life Sciences, The Natural History Museum, London SW7 5DB, United Kingdom

<sup>&</sup>lt;sup>5</sup>Institut Universitaire de France (IUF), Paris, 75231, France

<sup>&</sup>lt;sup>6</sup>Staatliches Museum für Naturkunde Stuttgart, DE-70191, Germany

<sup>\*</sup>Corresponding author: Museo de Historia Natural, Universidad Nacional Mayor de San Marcos, Av. Arenales 1256, Jesús María, Lima 15072, Peru. Email: druelasp@unmsm.edu.pe

(iv) las variables bioclimáticas muestran correlaciones significativas con las proporciones de los huesos turbinados respiratorios y olfativos. Por lo tanto, nuestros resultados se alinean con la hipótesis general de que los huesos turbinados respiratorios más grandes pueden ayudar a afrontar condiciones ambientales adversas. Sin embargo, la relación entre la elevación y el área de la superficie de los huesos turbinados olfatorios sigue siendo un enigma. Varios otros factores ecológicos confusos que parecen estar presentes son discutidos. En general, este estudio provee información sobre las adaptaciones complejas de los huesos turbinados y sus interacciones con factores ambientales, contribuyendo a nuestro entendimiento de la ecomorfología de mamíferos en hábitats de bosque montano.

Palabras clave: Andes, bosque montano, conservación de calor y humedad, olfacción, Sigmodontinae.

The study of anatomical adaptations in response to environmental factors is a cornerstone of evolutionary biology. Turbinal bones in the nasal cavity of tetrapods, particularly in mammals, are complex structures with a dual role in heat and moisture conservation, and olfaction (e.g., Parsons 1967; Schmidt-Nielsen et al. 1970; Hillenius 1992; Green et al. 2012; Martinez et al. 2024a). These structures can be subdivided into 2 primary functional compartments (Fig. 1): (i) the anterior part, which contains the respiratory turbinals that warm and moisten inspired air before reaching the lungs, thereby optimizing respiratory efficiency; and (ii) the posterior part, which contains the olfactory turbinals involved in olfaction through their olfactory epithelium and connection to the olfactory bulb (e.g., Schmidt-Nielsen et al. 1970; Green et al. 2012; Smith et al. 2012; Pang et al.

2016; Martinez et al. 2024a, 2024b). Due to these combined roles, turbinal bones have emerged as potential ecological proxies for inferring the dietary habits and other ecological habits of mammals (e.g., Van Valkenburgh et al. 2011, 2014; Green et al. 2012; Martinez et al. 2024a). Exploring the complexities of turbinals not only unveils the complexity of physiological processes but also provides a unique perspective on how environmental conditions act as strong selective pressures driving evolutionary change (Green et al. 2012; Martinez et al. 2024a). Some studies have suggested a link between the relative surface area of the respiratory turbinals and environmental conditions linked to elevation and latitude, although none have rigorously tested this hypothesis (Van Valkenburgh et al. 2011, 2014; Green et al. 2012; Martinez et al. 2020).

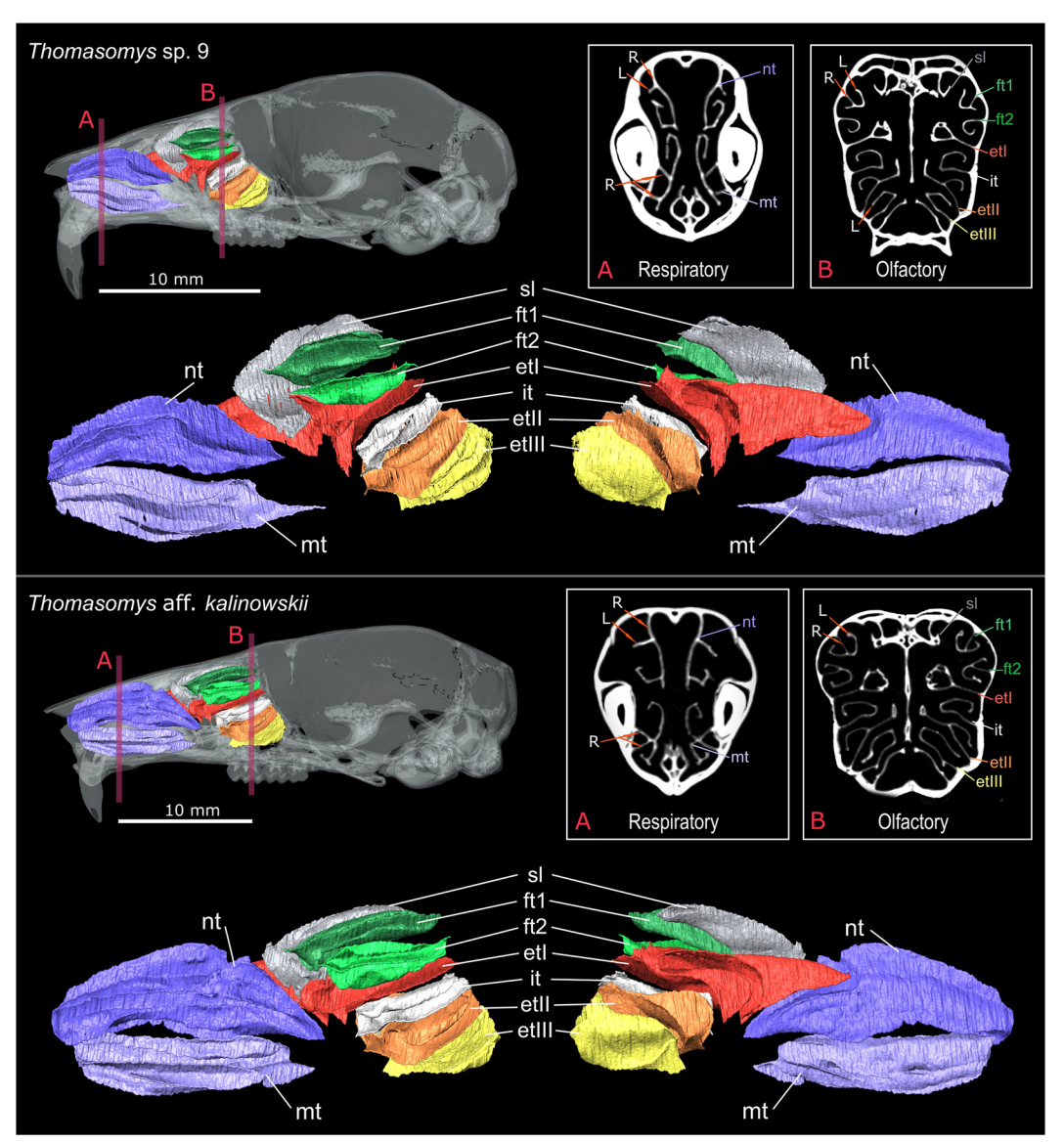


Fig. 1. Sagittal plane of the skull and coronal cross-section and 3D representations of turbinal bones (respiratory and olfactory) of Thomasomys sp. 9 and T. aff. kalinowskii. Abbreviations: R, root; L, lamella; nt, nasoturbinal; mt, maxilloturbinal; sl, semicircular lamina; ft1, frontoturbinal 1; ft2, frontoturbinal 2; it, interturbinal; etI, ethmoturbinal I; etII, ethmoturbinal II; etIII, ethmoturbinal III.

When examining the effects of elevation and environmental conditions, specialized functions of turbinals become particularly relevant. At higher elevations, the air is often less dense and cooler, with reduced oxygen levels, posing challenges for effective respiration and thermoregulation (Spence and Tingley 2020)—as such, selection related to habitat conditions would be expected to act mainly on respiratory turbinals more so than olfactory turbinals. Respiratory turbinals are mostly represented by the naso- and maxilloturbinal and are mostly covered by a highly vascularized respiratory epithelium composed of ciliated structures and mucus glands (Harkema et al. 2006; Barrios et al. 2014; Ruf 2020; Smith and Bonar 2022; Martinez et al. 2024a). As organisms adapt to these high-elevation conditions, changes in turbinal structure may occur to optimize respiratory efficiency. For example, the demands of heat and water retention are greater for species living at high elevations with cold and dry environments than those living at lower elevations with more temperate and mesic environments (Withers et al. 2016a, 2016b). Similarly, the olfactory turbinals underscore their significance in detecting scents, which can be vital for survival and reproduction (Moulton 1967; Green et al. 2012; Martinez et al. 2024a). Different environments may expose organisms to distinct odors, influencing their ability to find food, avoid predators, and communicate with conspecifics (Apfelbach et al. 2005; Martinez et al. 2024a). Therefore, studying how elevation and environmental conditions impact the structure and function of olfactory turbinals could contribute to our understanding of how animals adapt to their environment.

With its heterogeneous landscapes, the Andes offer an exceptional opportunity to study adaptive traits. Organisms inhabiting these regions have evolved a diverse array of morphological and physiological traits to cope with harsh conditions (Voss 1988; Monge and Leon-Velarde 1991; Rezende et al. 2005; Withers et al. 2016a; Schenk and Steppan 2018) such as high elevation, low temperature, and varying humidity (e.g., high in montane and premontane forests, low in puna). High-elevation species mainly face the dual challenges of colder temperatures and increased respiratory demands due to lower oxygen levels (Withers et al. 2016a, 2016b; Luna et al. 2017; Butaric and Klocke 2018). The Andean environments are home to a rich diversity of rodents (Patterson et al. 2012; Vallejos-Garrido et al. 2023), making them a prime group for investigating adaptive traits.

In the realm of Andean mammalian diversity, the Thomasomys genus stands out for its remarkable adaptability to varying high-elevational zones, exclusively inhabiting montane forests (including premontane forests) and paramos. The genus spans an impressive range of 3,350 m elevation (from 1,150 to 4,500 m) with most species inhabiting between 2,000 to 3,500 m (Supplementary Data SD1). These species generally have very limited distributional ranges (see maps and remarks in Pacheco 2015). The mean annual temperatures of these forests vary, with upper montane forests (2,500 to 3,500 m) experiencing 7 to 15 °C, and lower montane forests (1,500 to 2,500 m) 15 to 19 °C (Young and León 1999). Some localities can have minimum temperatures of 6.8 °C or less (Wright and Zegarra 2000; Llerena-Zambrano et al. 2021). Significantly, Thomasomys species are completely absent from certain geographic areas such as the Guiana Shield, lowland tropical forests, desert regions, and oceanic islands (Pacheco 2003, 2015; Pacheco et al. 2015). As the most diverse genus of sigmodontine rodents, Thomasomys includes 51 valid and several undescribed species (Pacheco 2015; Pacheco and Ruelas 2023; Ruelas et al. 2024). Many species co-occur within the same montane habitat, with up to 7 or 8 in the same locality, most exhibiting semi-arboreal or scansorial behavior (Leo and Gardner 1993; Voss 2003; Brito et al. 2012; Pacheco 2015). Morphologically, the genus spans a wide range, from the smaller T. daphne (head and body length = 80 mm) to the larger T. apeco (head and body length = 238 mm), with corresponding

weights varying from 14 to 335 g (Pacheco 2015; Supplementary Data SD2). Such distribution patterns and morphological diversity underline ecological specialization and adaptation to mountain niches in Thomasomys, with elevational gradients playing a crucial role in habitat selection. Unlike other diverse genera like Akodon (42 species) and Oligoryzomys (32 species)—which have fewer species confined to high-elevation forests (Pardiñas et al. 2015; Weksler and Bonvicino 2015; Brandão et al. 2021; Hurtado, D'Elía 2022)—Thomasomys thrives in these habitats, potentially linked to specific adaptations. In semiaquatic rodents, Martinez et al. (2020) suggested that respiratory turbinals may be larger in species living in colder habitats (mediated by elevation), indicating a temperature-adapted evolutionary response—a pattern that could represent convergent evolution in response to similar ecological pressures. The high morphological variation and diversity of Thomasomys underscore its adaptability to diverse environmental conditions, allowing it to exploit a broad range of resources. However, despite its ecological success, limited understanding of Thomasomys hinders the formulation of evolutionary hypotheses about its adaptation and radiation in high-elevation habitats. The diverse environmental conditions across Andean elevational gradients likely impose considerable selective pressures on Thomasomys morphology, driving their varied adaptations and ecological success.

Therefore, Thomasomys species present a model system for testing the hypothesis that mammals through high-elevation habitats may display distinct morphological adaptations specifically linked to their capacity to conserve heat and moisture. In this sense, we expect that Thomasomys species inhabiting higher elevations present larger respiratory turbinals due to their increased need for warm air. By using turbinal surfaces as a proxy for homeothermic function, our study aims to unravel the complex interplay between elevation, environmental variables, and morphological structures.

#### Methods

#### **Specimens**

We employed 45 adult specimens of Thomasomys species preserved in ethanol, representing 19 taxa (Appendix I). The use of ethanol-preserved specimens ensured that the anterior part of the respiratory turbinal is not damaged due to cleaning methods, which is an important factor for a quantitative approach at this taxonomic scale. These specimens were collected in Peru and Colombia between 1,500 and 3,380 m a.s.l. (Supplementary Data SD3 and SD4) and are housed in the Museum of Natural History of the Universidad Nacional Mayor de San Marcos (MUSM, Lima) and the Field Museum of Natural History (FMNH, Chicago). Species identification was made by D. Ruelas and V. Pacheco and taxonomic nomenclature follows Pacheco (2015) and Ruelas et al. (2024). Also, we downloaded CT scans of the skull of T. aureus (MEPN 6144) from MorphDbase (https://www.morphdbase.

In the absence of a multilocus phylogenetic hypothesis, we grouped Thomasomys species based on the morphological species groups proposed by Pacheco (2015) and the unilocus phylogeny findings of Ruelas et al. (2024). Our specimens fell into 6 species groups: Baeops group (n = 10) with small-sized species found at elevations from 1,500 to 2,950 m a.s.l.; Cinereus group (n=11) with small- and medium-sized species distributed from 2,200 to 3,290 m a.s.l.; Gracilis group (n=1), with small species at 2,880 m a.s.l.; Incanus group (n=11) with medium-sized species ranging from 2,200 to 3,380 m a.s.l.; and Notatus group (n=2) represented by the medium-sized T. notatus found between 1,900 and 1,920 m a.s.l. The Aureus group, mainly comprising large-sized species distributed from 2,117 to 3,217 m a.s.l, was divided into Aureus W (n=6) and Aureus E (n=4) based on the findings of

Ruelas et al. (2024; Fig. 2; Supplementary Data SD2 and SD4). The relative size of each species is given in Supplementary Data SD4.

## Data acquisition.

We acquired the 3D data using an EasyTom 150 microtomograph with a voxel size ranging from 0.018 to 0.027 mm. By using unstained ethanol-preserved specimens and classical CT technology, we were able to image only bony structures (high-density materials) and produce results comparable to most studies on turbinals, which primarily use dry skulls. We segmented only turbinals from the left side of the skull following Martinez et al. (2018) with Avizo Lite 9.0.1 (Fisher Scientific Inc., USA). In cases where the left side of the skull was damaged due to the use of snap traps for mouse collection, we segmented the right side. We manually segmented the turbinals every 2 or 3 images, and an interpolation was employed to bridge the gaps in segmentation—we then checked all interpolated images to correct any potential errors.

#### **Variables**

Explanatory variable sets were generated as follows:

#### Size

We extracted skull length (SL, in mm)—measured from the most anterior part of the nasal bone to the most posterior part of the occipital bone (Supplementary Data SD4) from the reconstructed CT data with Avizo Lite v. 9.0.1.

#### Turbinal surface area

We extracted the surface area of the segmented turbinals using Avizo Lite v. 9.0.1. (Supplementary Data SD4). We merged the turbinal surface areas (Fig. 1) into respiratory (naso- and maxilloturbinal) and olfactory (ethmoturbinals, interturbinal, and semicircular lamina) turbinals following the turbinal functional partitioning by Martinez et al. (2018, 2024a, 2024b). In rodents, the epithelial cover of the maxilloturbinal is widely accepted when measuring surface area (Martinez et al. 2024a, 2024b). While the nasoturbinal is predominantly covered by respiratory epithelium, there are limited comparative histology data and this covering can vary significantly among mammalian species (e.g., Smith and Bhatnagar 2004; Smith and Rossie 2008; Smith et al. 2012; Pang et al. 2016; Martinez et al. 2024a). Therefore, we separately analyzed the naso- and maxilloturbinal to evaluate the potential impact of this functional partitioning on our findings (see Martinez et al. 2018, 2020 for a similar methodology). Considering turbinal morphology, we used the terminology of Ito et al. (2022) and Martinez et al. (2024a, 2024b).

#### Elevation

We extracted these data (in meters) from the Museum collection databases. If elevation was not provided, it was estimated based on either the geographic coordinates or details of the location where the specimen was collected (Appendix I).

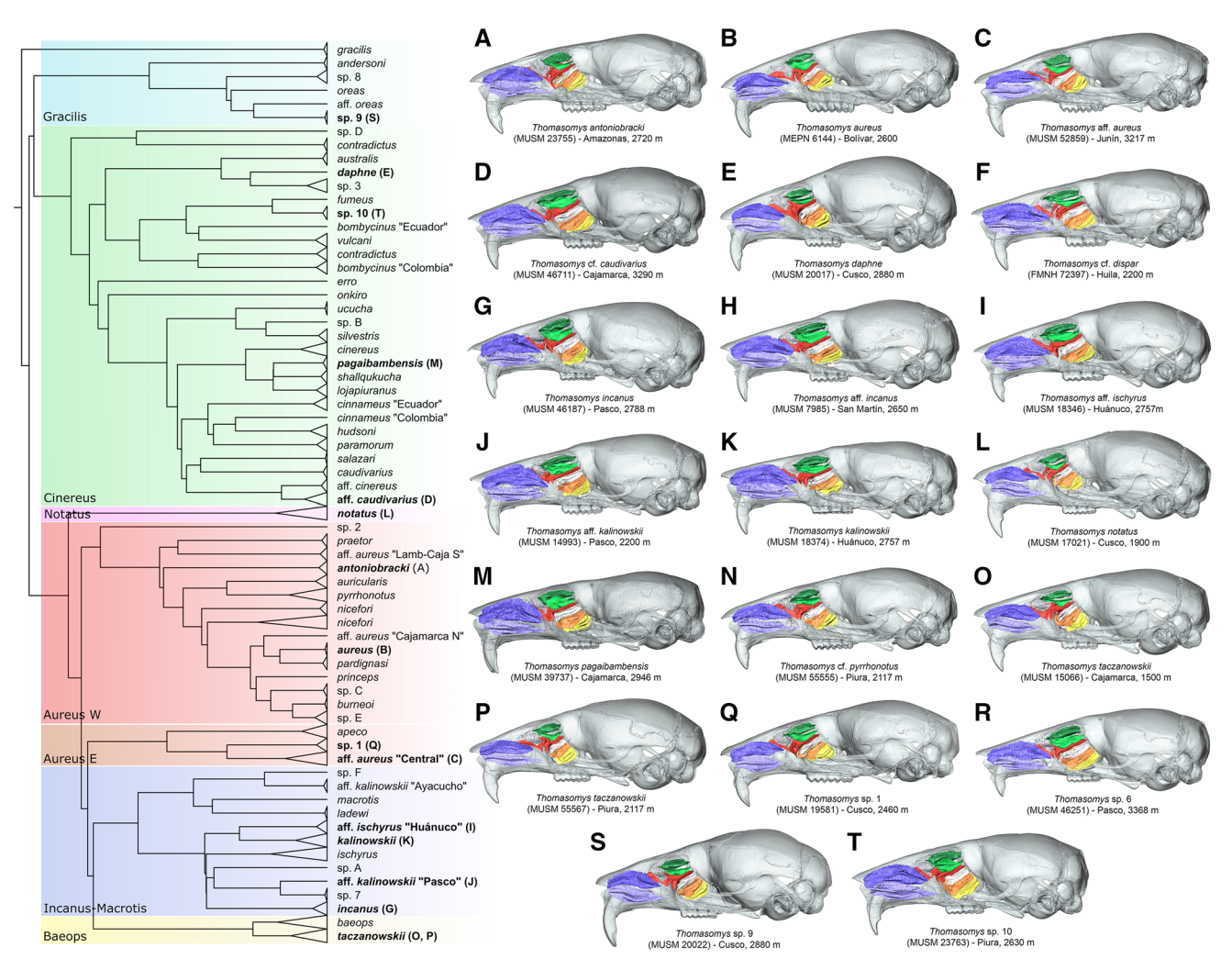


Fig. 2. Phylogeny and morphological diversity of the turbinal bones of Thomasomys species. The phylogenetic tree is derived from Ruelas et al. (2024) and associated with 3D representations of turbinal bones and coronal cross-section along the Thomasomys species used in this study (A-T).

#### Bioclimatic variables

We retrieved climatic data variables with a resolution of 2.5 arc-min from the WorldClim 2.1 database (https://www.worldclim.org) for the period of 1970 to 2000 (Fick and Hijmans 2017). The 19 bioclimatic variables available were retrieved as follows: BIO1=annual mean temperature; BIO2=mean diurnal range (mean of monthly [max temp—min temp]); BIO3=isothermality (BIO2/BIO7) (×100); BIO4=temperature seasonality (standard deviation ×100); BIO5=max temperature of warmest month; BIO6=min temperature of coldest month; BIO7=temperature annual range (BIO5-BIO6); BIO8=mean temperature of wettest quarter; BIO9=mean temperature of driest quarter; BIO10=mean temperature of warmest quarter; BIO11=mean temperature of coldest quarter; BIO12=annual precipitation; BIO13 = precipitation of wettest month; BIO14 = precipitation of driest month; BIO15=precipitation seasonality (coefficient of variation); BIO16 = precipitation of wettest quarter; BIO17 = precipitation of driest quarter; BIO18=precipitation of warmest quarter; and BIO19=precipitation of coldest quarter (Supplementary Data SD4).

#### Data correction.

In the study of turbinal structures, researchers commonly recommend 2 forms of correction to account for variations: sizing by overall body size using metrics including SL, body length, or mass and sizing by total turbinal surface area (TTSA; e.g., Green et al. 2012; Martinez et al. 2018, 2020). Our research employs both corrections to explore functional morphology and adaptive significance of turbinal structures

Sizing by body size allows for comparing morphological traits and shapes without size bias, facilitating the detection of differences and the investigation of evolutionary and ecological adaptations (e.g., Green et al. 2012; Porto et al. 2013; Weaver and Grossnickle 2020; Mitchell et al. 2024). Here, sizing by SL allows for proportional comparisons within the skull, allowing for testing of the hypothesis that larger turbinals may indicate adaptation to colder, high-elevation environments. For this, we performed a log-transformed standardized major axis (SMA) between SL as an independent variable and respiratory (RTSA), olfactory turbinal surface area (OTSA), and total TTSA as dependent variables (Warton et al. 2006; Green et al. 2012). The SMA results were used to test for allometric variation. The slope from the SMA model was tested against 1 to determine if the scaling was isometric (slope = 1) or allometric (slope ≠ 1). SMA is better for testing allometry because it symmetrically treats both variables, accommodates measurement errors, and accurately summarizes relationships on logarithmic scales (Warton et al. 2006).

Sizing by TTSA offers insight into the balance between respiratory and olfactory capabilities, offering insights into ecological and evolutionary adaptations (e.g., Martinez et al. 2018, 2020, 2023a). We hypothesized an adaptive trend toward larger respiratory and reduced olfactory proportions in response to colder, high-elevation environments, enhancing heat, and moisture conservation while possibly reducing olfactory sensitivity. To test for this, we performed log-transformed linear regressions between the TTSA as an independent variable and both RTSA and OTSA as dependent variables.

For our subsequent analyses, we used residuals from these analyses which are respectively referred to as (i) relative respiratory turbinal surface area (relative RTSA); (ii) relative olfactory surface area (relative OTSA); and (iii) relative total turbinal surface area (relative

# Phylogenetic correction.

We used a phylogenetic tree of the genus Thomasomys (Ruelas et al. 2024) in NEXUS format, retaining only species with available turbinal surface area data. For species lacking representation in the molecular

phylogeny including Thomasomys sp. 6, T. cf. pyrrhonotus, T. dispar, and Thomasomys sp. A, we provisionally placed them within the tree based on morphological and distributional affinities following Pacheco (2003, 2015) and Ruelas et al. (2024). These placements are tentative and designed to integrate these species into the phylogenetic framework until further molecular data become available to refine their positions. For species with multiple specimens, we calculated the average for SL, RTSA, OTSA, and TTSA. After aligning these data with the phylogenetic tree, we applied Phylogenetic Generalized Least Squares (PGLS) to account for evolutionary relationships (Martins and Hansen 1997; Revell 2012), fitting models for both RTSA and OTSA as functions of SL and TTSA. This method incorporates the evolutionary history of species into a generalized least squares framework, allowing phylogenetic correction to make more accurate inferences about trait correlations (Martins and Hansen 1997). We fitted PGLS models for both the respiratory and olfactory turbinal surface areas as a function of SL and TTSA. We tested 4 evolutionary models: (i) Brownian motion model, which assumes species evolve according to a random-walk process (Felsenstein 1985); (ii) OU (Ornstein-Uhlenbeck) model, which represents stabilizing selection or attraction to an optimum trait value (Butler and King 2004); (iii) Grafen model, which is a transformation of branch lengths based on a power scaling of evolutionary distances (Grafen 1989); and (iv) without phylogeny. We then used the Akaike Information Criterion (AIC) to compare these models and select the best fit. The model with the lowest AIC score, which balances model fit and complexity, was chosen for final interpretation (Burnham and Anderson 2004). For our subsequent analyses, we used residuals from the best models.

## Quantitative analyses.

To delve into the interplay between nasoturbinal and maxilloturbinal and between respiratory and olfactory turbinal surface areas of Thomasomys and their potential correlation after accounting for the size effect (SL sized), an initial step involved assessing the normality of the variables (relative surface areas), accomplished through the Shapiro-Wilk test. This test resulted in a non-normal distribution identified in both relative nasoturbinal (W=0.909, P=0.002) and maxilloturbinal (W=0.935, P=0.014) surface areas, as well as in the relative RTSA (W=0.949, P=0.045) and relative OTSA (W=0.929, P=0.009). Consequently, we used Kendall's Tau correlation coefficient for analysis, a method supported by Bolboacă and Jäntschi (2006) and Ghent (1963) for its effectiveness with non-normal data. This approach helps determine the extent to which changes in one variable are associated with changes in another (Jarantow et al. 2023).

To assess the influence of environmental factors (elevation and bioclimatic variables) on turbinal surface areas sized by SL, we conducted a multiple robust regression analysis (MM-regression analysis; Yohai 1987; Koller and Stahel 2011), given the non-normal SMA residuals. This method is an alternative to least squares regression and is less affected by outliers. Moreover, it handles non-normal errors, mitigates the influence of leverage points, and addresses heteroscedasticity better than ordinary least squares regression, making it more reliable for complex biological and environmental datasets (Yohai 1987; Lourenço et al. 2011; Koller and Stahel 2011; Bowlby and Gibson 2015). Conversely, for the data sized by TTSA, which displayed a normal distribution for both respiratory (W=0.985, P=0.807) and olfactory turbinals (W=0.982, P=0.691), we conducted multiple linear regressions. In these analyses, the relative surface areas of turbinals were defined as dependent variables, with elevation and bioclimatic variables as independent variables.

Then, to evaluate the relationship between turbinal surface areas and environmental factors, we analyzed the residuals from the AIC-selected phylogenetic models. This approach allowed us to assess whether environmental factors significantly shaped turbinal surface areas, independent of phylogeny (Freckleton et al. 2002). Because environmental variables are given in different scales, we used minimum and maximum values to represent elevation, and for bioclimatic variables (2.5 arc-min resolution), we calculated averages. Using these data, we tested 4 models using PGLS: (i) Brownian motion model; (ii) OU (Ornstein-Uhlenbeck) model; (iii) Grafen model; and (iv) with no phylogeny effect. We then used the AIC to compare these models and select the best fit. Finally, we used visualization techniques—including phenograms and phylogenetic plots—to map trait changes across phylogeny, and performed ancestral state reconstruction to illustrate trait evolution (Revell 2012).

For all analyses, we used the "ape" (Paradis and Schliep 2019), "devtools" (Wickham et al. 2022), "dplyr" (Wickham et al. 2023b), "DT" (Xie et al. 2024), "ggplot2" (Wickham et al. 2023a), "multcomp" (Hothorn et al. 2024), "nlme" (Pinheiro et al. 2024), "phytools" (Revell 2012), "reshape2" (Wickham 2020), "robustbase" (Maechler et al. 2024), "smatr" (Warton et al. 2018), "smplot2" (Min and Zhou 2021), and "writexl" (Ooms and McNamara 2024) packages within the R version 4.1.3 environment (R Core Team 2022) and RStudio (RStudio Team 2024).

#### **Results**

## Scaling of turbinal surface areas.

In Thomasomys, the turbinal bones are consistently arranged throughout species, showing 2 pairs of respiratory turbinals (nasoturbinal

and maxilloturbinal), located in the anterior portion of the rostrum, and 7 pairs of olfactory turbinals (semicircular lamina, frontoturbinal 1, frontoturbinal 2, ethmoturbinal I, interturbinal, ethmoturbinal II, and ethmoturbinal III) located more posteriorly within the nasal cavity (Fig. 1). Despite interspecific differences, these turbinals showed slightly conserved morphological patterns (Figs 1 and 2; Supplementary Data SD5 and SD6). A detailed morphological description is provided in Appendix II.

To explore the interplay between turbinal surface areas and SL, we generated an array of regression plots involving the 3 distinct categories: RTSA, OTSA, and TTSA. We found statistically significant correlations in each comparison, with RTSA (Adjusted R<sup>2</sup>=0.58, P=1.33e-09, S=2.92; Fig. 3A), OTSA (adjusted  $R^2=0.603$ , P=3.68e-10, S=2.64; Fig. 3B), and TTSA (adjusted  $R^2=0.611$ , P=2.32e-10, S=2.7; Fig. 3C) all showing positive allometric scaling since the slopes significantly deviate from 1 (isometry). Adjusted R2 values indicate a relatively strong relationship, indicating that a significant portion of the variance in turbinal surface areas is explained by SL. These findings underscore that, in general, large members of Thomasomys display similar or more developed turbinal surface areas when compared with their smaller counterparts (Fig. 3A-C; Supplementary Data SD7).

Interestingly, large Thomasomys species, such as T. antoniobracki (SL = 44.76 to 43.86 mm; occurring at 2,630 and 2,720 m) and T. aff. aureus (SL = 40.58 to 40.85 mm; occurring at 3,217 m), respectively from the Aureus E and W groups, display less developed turbinal surface areas when compared with smaller species like T. taczanowskii from the Baeops group (SL = 26.94 to 29.63; found between 1,500 and 2,950 m;

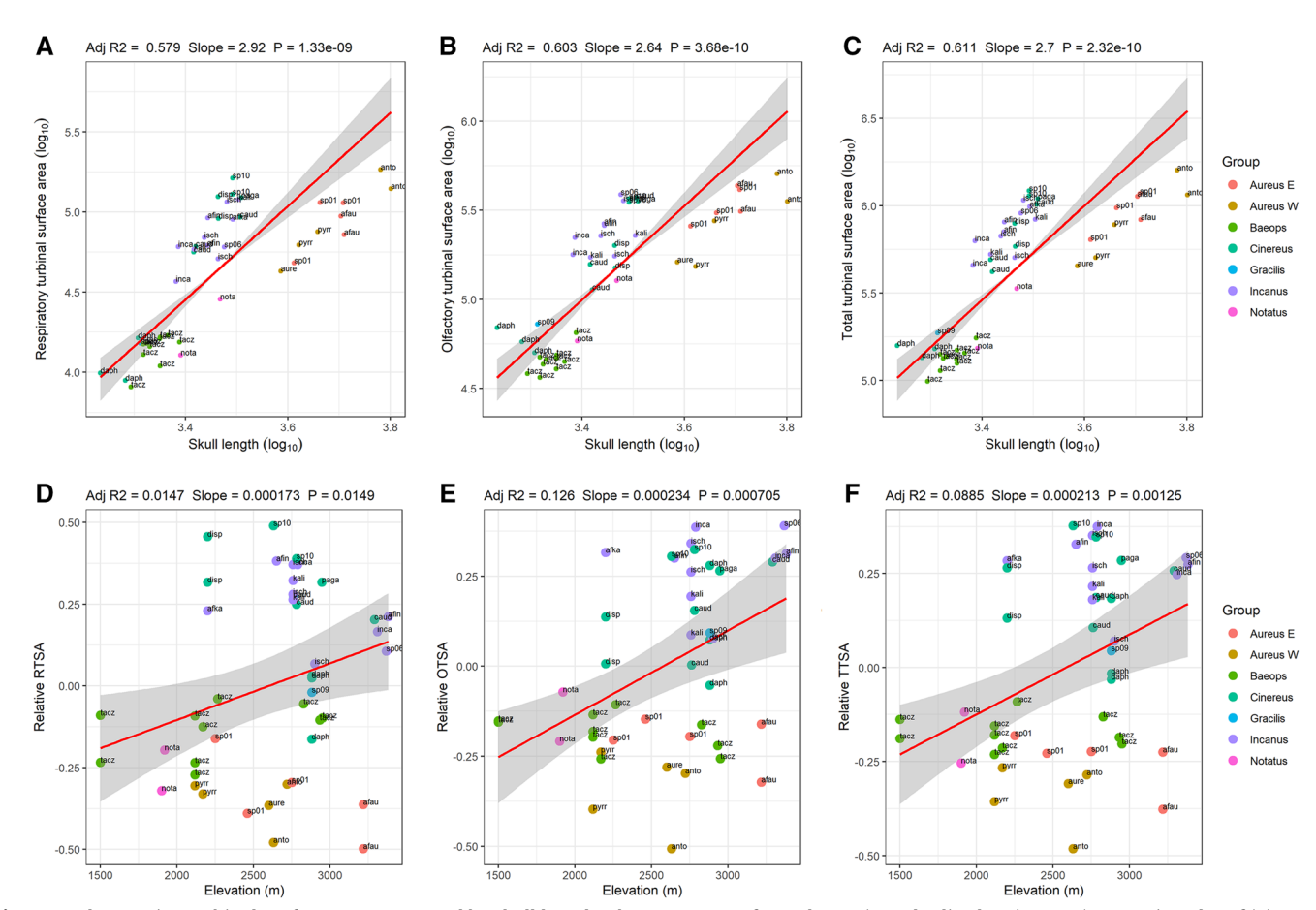


Fig. 3. Analyses using turbinal surface areas corrected by skull length. Above: Log-transformed SMA (Standardized Major Axes) regression plot of (A) respiratory turbinal surface area against skull length, (B) olfactory turbinal surface area against skull length, and (C) total turbinal surface area against skull length. Below: Multiple robust regressions of (D) relative respiratory turbinal surface area (RTSA) against elevation, (E) relative olfactory turbinal surface area (OTSA) against elevation, and (F) relative total turbinal surface area (TTSA) against elevation. Colors represent the species groups sensu Pacheco (2015). Abbreviations for species are listed in Supplementary Data SD4.

Fig. 3). It is also interesting to note that some mid-sized species of the Cinereus group including T. sp. 10 (SL = 32.85 mm; occurring at 2,630 and 2,780 m) and T. pagaibambensis (SL = 33.43 mm; occurring at 2,946 m), and Incanus group, including T. kalinowskii (SL = 30.47 to  $33.25 \,\mathrm{mm}$ ; inhabiting at  $2,757 \,\mathrm{m}$ ) and T. ischyrus (SL =  $31.09 \,\mathrm{to}$ 32.05 mm; inhabiting at 2,757 and 2,900 m)—occurring at similar elevations but different localities—showed turbinal surface areas comparatively as large as the large-sized species (Fig. 2; Supplementary Data SD4 and SD7). Moreover, we did not uncover a direct correlation between SL—as a proxy for body size—and elevation, indicating that Thomasomys species of various sizes coexist across a similar elevation range, specifically between 2,000 and 3,000 m (Supplementary Data SD7 and SD8). This distribution pattern is evident across different Thomasomys groups, including Aureus E, Aureus W, Baeops, Cinereus, and Incanus—highlighting a complex relationship between size and other factors beyond the influence of elevation alone.

Using phylogenetic correction, the analysis showed that the best-fitting model for the RTSA as a function of SL was the Grafen model (AIC: -9.502, P<0.001), suggesting that evolutionary history significantly influences this trait. For OTSA as a function of SL, the Brownian motion model provided the best fit (AIC: -8.694, P=0.0002), suggesting a random and gradual evolutionary pattern. However, when analyzing both RTSA and OTSA as functions of TTSA, models without phylogenetic correction were chosen (RTSA, AIC=-33.544, P<0.001; OTSA, AIC=-51.871, P<0.001), suggesting that these relationships are primarily shaped by direct morphological scaling rather than phylogeny.

#### Correlation analysis.

Through correlation analyses, we found that after accounting for the size effect by SMA, there is a positive correlation between the relative nasoturbinal and maxilloturbinal surface areas (tau = 0.746, P=4.441e-16) and between the relative respiratory and olfactory turbinal surface areas (tau = 0.624, P = 0.009). These findings underscore that smaller nasoturbinals are associated with smaller maxilloturbinals (Fig. 4A; Supplementary Data SD5). Smaller relative RTSA in Thomasomys species like T. taczanowskii tend to coincide with smaller OTSA (Fig. 4B; Supplementary Data SD5); while species with larger RTSA like Thomasomys sp. 10, T. ischyrus, or T. aff. incanus, exhibit larger OTSA. Notably, larger species in the Aureus W group and smaller

species in the Baeops group consistently showed smaller turbinal surface areas in both nasoturbinals and maxilloturbinals, as well as RTSA and OTSA. Conversely, mid-sized species of the Cinereus and Incanus groups displayed more extensive turbinals. Overall, our results suggest an absence of an evolutionary trade-off between the naso- and maxilloturbinals, as well as between the respiratory and olfactory turbinals.

#### Influence of elevation.

Remarkably, when considering SL as a sizing factor, elevation displays a statistically significant but slightly weak positive relationship with relative RTSA (Adjusted  $R^2 = 0.015$ , P = 0.015; Fig. 3D), while relative OTSA exhibits a stronger and significant positive correlation with elevation (adjusted  $R^2 = 0.126$ , P = 0.001; Fig. 3E), meaning a clear trend where species inhabiting lower-elevation habitats often display smaller relative RTSA and OTSA (Supplementary Data SD6). Moreover, there is a statistically significant, positive relationship between elevation and TTSA (adjusted  $R^2 = 0.089$ , P = 0.001; Fig. 3F). Species groups with the widest elevation range, such as the Cinereus and Incanus groups, exhibited a dispersed pattern in the analysis involving RTSA (Fig. 3A), while their OTSA showed a slightly increasing trend (Fig. 3B). However, for the other groups, the relationship between RTSA or OTSA and elevation was not as evident. Together, these findings highlight the notable influence of elevation on the complex morphological attributes of turbinal surface areas within Thomasomys species. On the other hand, species size does not seem to correlate with elevation (Supplementary Data SD8), indicating that diverse sizes of Thomasomys species coexist within the same elevation ranges. However, when considering TTSA as the sizing factor (Fig. 5A-B), the correlation between elevation and both relative RTSA (adjusted R2 = 0.050, P=0.075; Fig. 5C) and relative OTSA (adjusted  $R^2 = 0.046$ , P=0.085; Fig. 5D) was not statistically significant. This result may indicate that while elevation influences turbinal surface areas, other factors might play crucial roles in shaping the proportion of respiratory and olfactory turbinals with the rostrum.

When considering phylogenetic correction scaled for SL, the OTSA and minimum elevation showed a significant positive correlation (P=0.026). Contrarily, no significant relationships were found for the RTSA with either minimum or maximum elevation (Table 2; Supplementary Data SD9). Moreover, when examining RTSA and OTSA as

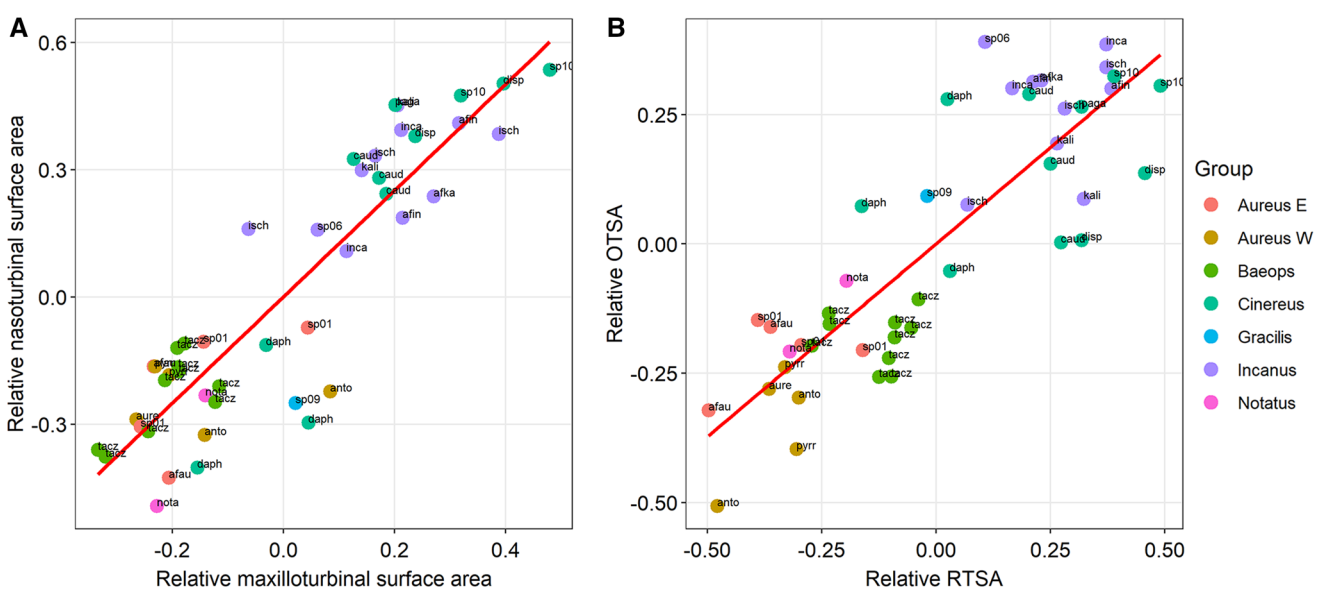


Fig. 4. Plots of Kendall's tau correlation between (A) residuals of nasoturbinal and maxilloturbinal surface areas and (B) residuals of olfactory (OTSA) and respiratory (RTSA) turbinal surface areas of Thomasomys. Colors represent species groups sensu Pacheco (2015). Abbreviations for species are listed in Supplementary Data SD4.

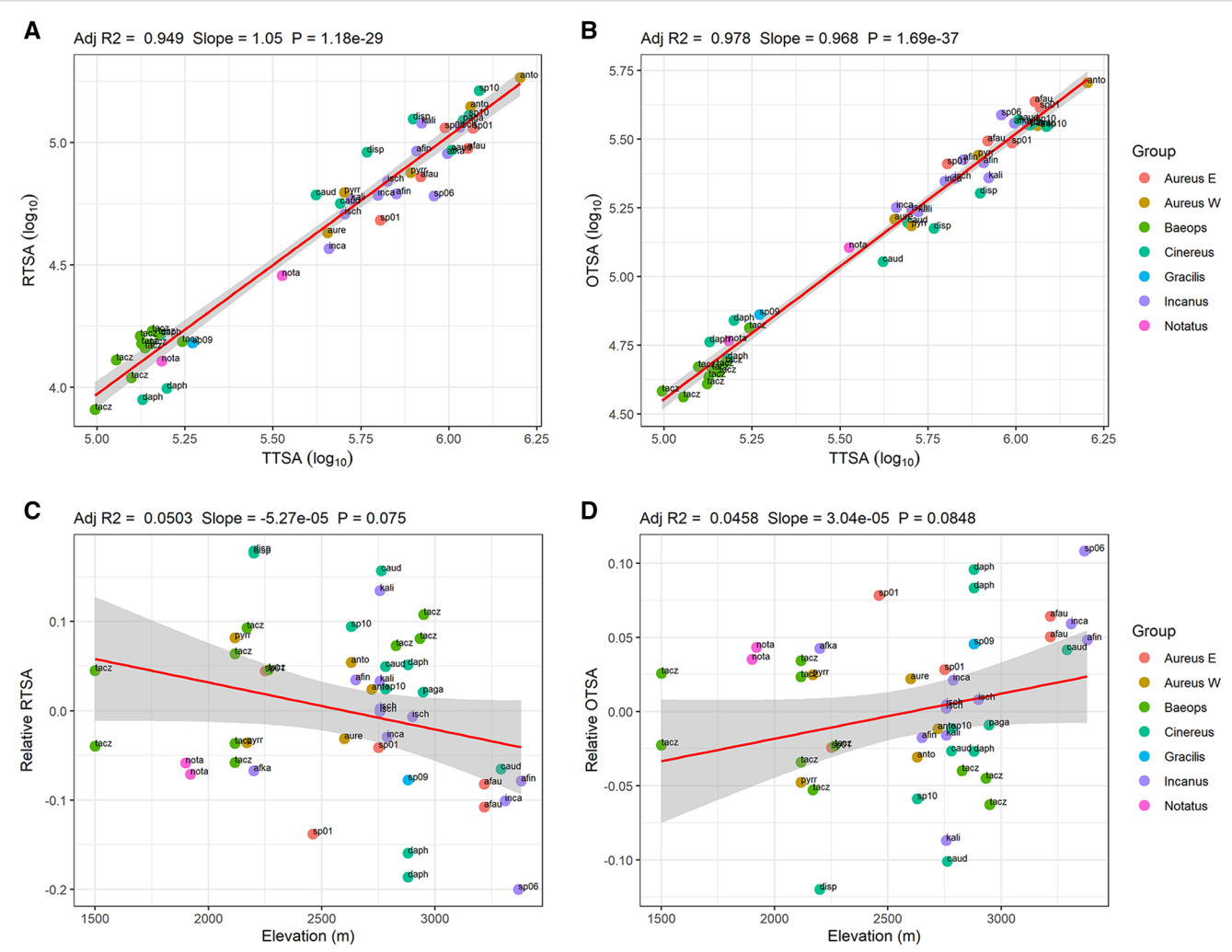


Fig. 5. Analyses using turbinal surface areas corrected by total turbinal surface area (TTSA). Above: Log-log linear regressions (red line) of (A) respiratory turbinal surface area (RTSA) against TTSA, (B) olfactory turbinal surface area (RTSA) against TTSA. Below: Linear regressions of (C) relative RTSA against elevation, (D) relative OTSA against elevation. Colors represent species groups sensu Pacheco (2015). Abbreviations for species are listed in Supplementary Data SD4.

functions of TTSA, neither minimum nor maximum elevation showed significant correlations, suggesting that elevation alone may not be a primary driver for turbinal adaptations (Table 3; Supplementary Data SD10).

#### Influence of bioclimatic variables.

The linear regression results showed varying associations between bioclimatic variables and the relative turbinal surface areas (RTSA, OTSA, and TTSA) in Thomasomys species (Table 1). When scaling by SL, a slight correlation was observed between BIO12 (annual precipitation, P=0.041), BIO14 (precipitation of driest month, P=0.021), BIO15 (precipitation seasonality, P=0.019), and BIO18 (precipitation of warmest quarter, P=0.040). No significant correlations were found in the other comparisons. Remarkably, there is no significant correlation between these environmental variables and elevation ( $P_{\text{BIO}12} = 0.3299$ ,  $P_{BIO14} = 0.365$ ,  $P_{BIO15} = 0.243$ ,  $P_{BIO18} = 0.0623$ ; Supplementary Data SD11).

Significant correlations were found between most bioclimatic variables and the relative RTSA and relative OTSA when sized by TTSA, with exceptions for temperature-related variables, including BIO05 (maximum temperature of warmest month;  $P_{RTSA} = 0.411$ ,  $P_{OTSA} =$ 0.491); BIO8 (mean temperature of wettest quarter;  $P_{RTSA} = 0.079$ ,  $P_{OTSA}$ = 0.101); BIO10 (mean temperature of warmest quarter;  $P_{RTSA}$ = 0.116,  $P_{\text{OTSA}}$  = 0.141); and BIO01 (annual mean temperature;  $P_{\text{OTSA}}$  = 0.052) but only for relative OTSA (Table 1). These results suggest a complex relationship between proportions of the turbinal surface areas and environmental factors, suggesting that temperature-related variables may have a less noticeable effect on turbinal morphology compared to other bioclimatic factors.

When incorporating phylogenetic correction and using turbinal surface area residuals as a function of SL, we only found a significant correlation between relative RTSA and temperature seasonality (BIO04, P=0.038) under the Grafen model (Table 2; Supplementary Data SD9). No other significant correlations were found in the other comparisons using residuals of RTSA and OTSA. In contrast, using turbinal surface area residuals as a function of TTSA, we found several significant correlations between relative RTSA and 9 bioclimatic variables under the no-phylogeny model including mean diurnal range (BIO02, P=0.013), isothermality (BIO03, P=0.002), temperature seasonality (BIO04, P=0.021), minimum temperature of the coldest month (BIO06, P=0.012), temperature annual range (BIO07, P=0.006), annual precipitation (BIO12, P=0.024), precipitation of the driest month (BIO14, P=0.002), precipitation seasonality (BIO15, P=0.004), precipitation of the driest quarter (BIO17, P=0.001), and precipitation of the coldest quarter (BIO19, P=0.001) (Table 3; Supplementary Data SD10). For relative OTSA as a function of TTSA, we found a significant correlation for temperature seasonality (BIO04, P=0.023) under the OU model. Under the no-phylogeny model, 9 significant correlations were found, including mean diurnal range (BIO02, P=0.010),

Downloaded from https://academic.oup.com/jmammal/advance-article/doi/10.1093/jmammal/gyaf061/8253798 by KIM Hohenheim user on 20 September 2025

Table 1. Results of the multiple robust regression of the relative turbinal surface areas (RTSA: Respiratory turbinal surface area, OTSA: Olfactory turbinal surface area and OTSA) sized by Skull length and Linear regression of the relative turbinal surface areas (RTSA and OTSA) sized by Skull length and Linear regression of the relative turbinal surface areas (RTSA and OTSA) sized by Skull length and Linear regression of the relative turbinal surface areas (RTSA and OTSA) sized by Skull length and Linear regression of the relative turbinal surface areas (RTSA and OTSA) sized by Skull length and Linear regression of the relative turbinal surface areas (RTSA and OTSA) sized by Skull length and Linear regression of the relative turbinal surface areas (RTSA and OTSA) sized by Skull length and Linear regression of the relative turbinal surface areas (RTSA and OTSA) sized by Skull length and Linear regression of the relative turbinal surface areas (RTSA and OTSA) sized by Skull length and Linear regression of the relative turbinal surface areas (RTSA and OTSA) sized by Skull length and Linear regression of the relative turbinal surface areas (RTSA and OTSA) sized by Skull length and Linear regression of the relative turbinal surface areas (RTSA and OTSA) sized by Skull length and Linear regression of the relative turbinal surface areas (RTSA) sized by Skull length and Skull length an

Bioclimatic Multiple robust regression	Multiple K	Multiple robust regression	sion							Linear regression	ression				
variables	Relative RTSA	TSA		Relative OTSA	TSA		Relative TTSA	TSA		Relative RTSA	TSA		Relative OTSA	TSA	
	Slope	Adj R2	P-value	Slope	Adj R2	P-value	Slope	Adj R2	P-value	Slope	Adj R2	P-value	Slope	Adj R2	P-value
BIO01	0.018	-0.031	0.451	-0.005	-0.046	0.813	0.002	-0.047	0.923	0.014	0.074	0.039	-0.008	0.064	0.052
BIO02	-0.032	-0.029	0.403	0.027	-0.027	0.377	0.004	-0.047	0.910	-0.038	0.238	4.0E-04	0.023	0.247	3.1E-04
BIO03	0.010	-0.005	0.137	-0.006	-0.028	0.339	0.000	-0.048	0.995	0.010	0.384	3.4E-06	-0.006	0.375	4.7E-06
BIO04	-0.002	0.013	0.063	0.000	-0.047	0.871	-0.001	-0.041	0.498	-0.001	0.260	2.1E-04	0.001	0.245	3.2E-04
BIO05	0.007	-0.044	0.792	-0.002	-0.048	0.928	0.000	-0.048	0.984	900.0	-0.007	0.411	-0.003	-0.012	0.491
BIO06	0.015	-0.020	0.291	-0.010	-0.032	0.445	-0.001	-0.048	0.934	0.016	0.261	2.0E-04	-0.009	0.245	3.2E-04
BIO07	-0.021	-0.016	0.230	0.013	-0.030	0.393	0.000	-0.048	666.0	-0.021	0.307	4.7E-05	0.013	0.306	4.8E-05
BIO08	0.008	-0.043	0.750	-0.012	-0.041	0.619	900.0-	-0.047	0.811	0.012	0.048	0.079	-0.007	0.039	0.101
BIO09	0.020	-0.019	0.287	-0.005	-0.045	0.782	0.004	-0.046	0.849	0.016	0.136	0.007	-0.009	0.123	0.011
BIO10	0.015	-0.035	0.543	-0.003	-0.047	0.892	0.002	-0.047	0.916	0.011	0.034	0.116	-0.006	0.028	0.141
BIO11	0.021	-0.018	0.267	-0.005	-0.046	0.801	0.004	-0.046	0.824	0.016	0.136	0.007	-0.009	0.122	0.011
BIO12	0.000	0.027	0.041	0.000	-0.048	0.839	0.000	-0.031	0.262	0.000	0.217	0.001	0.000	0.231	4.9E-04
BIO13	0.001	-0.029	0.381	-0.001	-0.037	0.531	0.000	-0.048	0.988	0.001	0.177	0.002	-0.001	0.166	0.003
BIO14	0.003	0.019	0.021	0.000	-0.046	0.752	0.001	-0.041	0.433	0.002	0.283	1.0E-04	-0.001	0.317	3.4E-05
BIO15	-0.006	0.024	0.019	-0.001	-0.047	0.773	-0.003	-0.031	0.221	-0.003	0.171	0.003	0.002	0.198	0.001
BIO16	0.000	-0.024	0.319	0.000	-0.044	0.737	0.000	-0.047	0.772	0.000	0.144	9000	0.000	0.140	0.007
BIO17	0.001	0.003	0.085	0.000	-0.040	0.545	0.000	-0.046	869.0	0.001	0.300	5.9E-05	0.000	0.336	1.8E-05
BIO18	0.001	0.022	0.040	0.000	-0.048	0.898	0.000	-0.033	0.305	0.000	0.196	0.001	0.000	0.200	0.001
BIO19	0.001	-0.014	0.229	0.000	-0.032	0.418	0.000	-0.048	0.944	0.001	0.287	8.9E-05	0.000	0.317	3E-05

Significant P-values are shown in bold. Abbreviations are explained in Methods.

Table 2. Results of the PGLS between the residuals of the respiratory turbinal surface area (RTSA) and the olfactory turbinal surface area (OTSA) as functions of skull length (SL) with elevation and bioclimatic variables.

Variable	RTSA					OTSA					
	Best Model	AIC	Intercept	Slope	P-value	Best Model	AIC	Intercept	Slope	P-value	
Min elevation	Grafen	-8.825	-0.033	0.000	0.842	Brownian	-14.444	-0.453	0.000	0.026	
Max elevation	Grafen	-8.792	-0.012	0.000	0.914	Brownian	-10.378	-0.276	0.000	0.228	
BIO01	Grafen	-8.817	-0.022	0.002	0.856	Brownian	-8.940	0.100	-0.007	0.646	
BIO02	Grafen	-9.869	0.403	-0.033	0.332	Brownian	-9.112	-0.287	0.024	0.548	
BIO03	Grafen	-12.195	-1.071	0.013	0.086	Brownian	-9.046	0.396	-0.005	0.582	
BIO04	Grafen	-13.775	0.190	-0.003	0.038	Brownian	-8.724	-0.015	0.000	0.872	
BIO05	Grafen	-8.780	0.016	0.000	0.969	Brownian	-8.867	0.122	-0.006	0.700	
BIO06	Grafen	-9.371	-0.035	0.007	0.475	Brownian	-9.215	0.051	-0.009	0.503	
BIO07	Grafen	-11.233	0.400	-0.026	0.146	Brownian	-9.019	-0.158	0.011	0.597	
BIO08	Grafen	-8.782	-0.002	0.001	0.957	Brownian	-8.980	0.113	-0.008	0.620	
BIO09	Grafen	-8.961	-0.051	0.004	0.692	Brownian	-8.972	0.095	-0.007	0.625	
BIO10	Grafen	-8.782	-0.002	0.001	0.956	Brownian	-8.923	0.102	-0.007	0.657	
BIO11	Grafen	-8.978	-0.053	0.005	0.678	Brownian	-8.964	0.094	-0.007	0.630	
BIO12	Grafen	-9.820	-0.078	0.000	0.343	Brownian	-8.785	-0.037	0.000	0.780	
BIO13	Grafen	-10.063	-0.111	0.001	0.293	Brownian	-9.026	-0.081	0.001	0.593	
BIO14	Grafen	-9.256	-0.019	0.001	0.521	Grafen	-9.107	0.038	-0.002	0.098	
BIO15	Grafen	-9.309	0.095	-0.002	0.499	Brownian	-8.975	-0.106	0.002	0.623	
BIO16	Grafen	-9.755	-0.101	0.000	0.359	Brownian	-9.129	-0.097	0.000	0.540	
BIO17	Grafen	-9.199	-0.019	0.000	0.547	Grafen	-9.164	0.043	-0.001	0.095	
BIO18	Grafen	-10.283	-0.109	0.000	0.255	Brownian	-9.119	-0.081	0.000	0.545	
BIO19	Grafen	-9.227	-0.021	0.000	0.534	Brownian	-9.112	0.044	0.000	0.549	

The best-fitting model for each variable is indicated, along with the AIC value, intercept, slope, and P-value. Significant correlations (P<0.05) are in bold.

Table 3. Results of the PGLS between the residuals of the respiratory turbinal surface area (RTSA) and the olfactory turbinal surface area (OTSA) as functions of total turbinal surface area (TTSA) with elevation and bioclimatic variables.

Variable	RTSA					OTSA					
	Best Model	AIC	Intercept	Slope	P-value	Best Model	AIC	Intercept	Slope	P-value	
Min	No phylogeny	-37.218	0.198	0.000	0.075	No phylogeny	-55.153	-0.113	0.000	0.093	
elevation											
Max	No phylogeny	-35.538	0.170	0.000	0.190	No phylogeny	-53.957	-0.104	0.000	0.180	
elevation											
BIO01	OU	-35.198	-0.154	0.011	0.230	OU	-53.380	0.088	-0.007	0.255	
BIO02	No phylogeny	-40.771	0.464	-0.039	0.013	No phylogeny	-59.499	-0.285	0.024	0.010	
BIO03	No phylogeny	-45.172	-0.887	0.011	0.002	No phylogeny	-63.650	0.536	-0.006	0.001	
BIO04	No phylogeny	-39.731	0.078	-0.001	0.021	OU	-57.901	-0.048	0.001	0.023	
BIO05	OU	-33.761	-0.083	0.004	0.652	OU	-52.028	0.040	-0.002	0.716	
BIO06	No phylogeny	-40.859	-0.098	0.016	0.012	No phylogeny	-58.835	0.058	-0.010	0.014	
BIO07	No phylogeny	-42.240	0.313	-0.022	0.006	No phylogeny	-60.827	-0.191	0.013	0.005	
BIO08	No phylogeny	-34.777	-0.143	0.010	0.303	OU	-52.958	0.079	-0.006	0.334	
BIO09	No phylogeny	-36.625	-0.186	0.014	0.103	OU	-54.710	0.105	-0.008	0.118	
BIO10	OU	-34.516	-0.126	0.009	0.356	OU	-52.753	0.071	-0.005	0.384	
BIO11	OU	-36.550	-0.180	0.014	0.106	OU	-54.655	0.104	-0.008	0.122	
BIO12	No phylogeny	-39.430	-0.135	0.000	0.024	No phylogeny	-58.632	0.086	0.000	0.016	
BIO13	No phylogeny	-36.769	-0.125	0.001	0.095	No phylogeny	-55.053	0.074	0.000	0.098	
BIO14	No phylogeny	-44.933	-0.079	0.002	0.002	No phylogeny	-65.492	0.050	-0.002	0.001	
BIO15	No phylogeny	-43.082	0.267	-0.005	0.004	No phylogeny	-63.370	-0.172	0.003	0.002	
BIO16	No phylogeny	-36.087	-0.118	0.000	0.139	No phylogeny	-54.521	0.072	0.000	0.131	
BIO17	No phylogeny	-45.540	-0.081	0.001	0.001	No phylogeny	-66.100	0.052	0.000	0.000	
BIO18	No phylogeny	-37.048	-0.116	0.000	0.082	No phylogeny	-55.944	0.075	0.000	0.061	
BIO19	No phylogeny	-45.841	-0.083	0.001	0.001	No phylogeny	-66.047	0.052	0.000	0.000	

The best-fitting model for each variable is indicated, along with the AIC value, intercept, slope, and P-value. Significant correlations (P<0.05) are in bold.

isothermality (BIO03, P=0.001), minimum temperature of the coldest month (BIO06, P=0.014), temperature annual range (BIO07, P=0.005), annual precipitation (BIO12, P=0.016), precipitation of the driest month (BIO14, P=0.001), precipitation seasonality (BIO15, P=0.002), precipitation of the driest quarter (BIO17, P<0.001), and precipitation

of the coldest quarter (BIO19, P < 0.001). These results suggest that both temperature and precipitation factors have considerable influence on variation in the proportions (respiratory and olfactory) of turbinal surface areas in Thomasomys species (Table 3; Supplementary Data SD10).

## **Discussion**

## High-elevation adaptations.

High-elevation adaptations in small mammals have been primarily studied through physiological responses, such as metabolic rate (e.g., Schippers et al. 2012; Arias-Reyes et al. 2021), breathing (e.g., Arias-Reyes et al. 2021), blood oxygen-carrying capacity (e.g., Tufts et al. 2013; Lui et al. 2015; Arias-Reyes et al. 2021), and water loss (e.g., Cortés et al. 1990, 2003; Withers et al. 2016b)—this study provides the first statistical evidence of adaptation using turbinal surface areas as a proxy of heat and moisture conservation in high-elevation environments. Specifically, we found a significant positive correlation between relative RTSA—when scaled by SL—and elevation (Fig. 3A; Supplementary Data SD6), supporting the hypothesis that species at higher elevation develop some morpho-physiological adaptation to minimize heat loss and to cope with harsh environmental conditions (Green et al. 2012; Withers et al. 2016b; Martinez et al. 2020, 2024a).

Large respiratory turbinals such as those in Thomasomys, with increased epithelial surface area and covered in moist mucous membranes, likely play a critical role in warming inhaled air and regulating moisture in high-elevation environments (Van Valkenburgh et al. 2004, 2014; Withers et al. 2016a, 2016b; Yuk et al. 2023). These adaptations enhance survival and success of species in Thomasomys, a genus that predominantly inhabits diverse high-elevation forests, mainly up to 2,000 m (Supplementary Data SD1). Their evolutionary success in colonizing and diversifying in these high-elevation forests during the Pliocene (Parada et al. 2015) further highlights their efficient adaptation to such environments. Our findings further found that Thomasomys species at higher elevations, such as T. caudivarius at 3,290 m and T. aff. incanus at 3,380 m, have significantly larger (size adjusted) and more complexly scrolled respiratory turbinals compared to their lower-elevation counterparts like T. taczanowskii from Cajamarca (1,500 m), suggesting morphological adaptation to highelevation conditions (Fig. 3; Supplementary Data SD6). In addition, mid-sized Thomasomys species at higher elevations may exhibit a more efficient respiratory system due to their relatively well-developed RTSA (Fig. 3D–F). This enhanced surface area likely facilitates the warming of inhaled air, which is essential in high-elevation environments. Similar mechanisms involving the use of maxilloturbinals to warm inhaled air for body temperature regulation have been reported in other mammals, including rabbits and some rodents (e.g. Jackson and Schmidt-Nielsen 1964; Schmidt-Nielsen et al. 1970; Caputa 1979; Xi et al. 2023).

Interestingly, we found a significant positive correlation between relative OTSA, adjusted for phylogenetic scaling, and minimum elevation under the Brownian motion model suggesting an elevation-related olfactory adaptation in Thomasomys (Table 2). This result suggests that OTSA evolves gradually along the phylogenetic tree (Supplementary Data SD9). Additionally, within a phylogenetic context, OTSA adjusted for SL showed a positive correlation with elevation (Fig. 3). In mammals, olfactory adaptations are often linked to ecological factors such as habitat complexity, diet, and behavior rather than elevation alone (Barton 2006; Martinez et al. 2024a). This finding suggests that olfactory capabilities in Thomasomys may be shaped not only by elevation but also by a broader set of ecological factors that vary with altitude such as resource availability, vegetation complexity, and environmental predictability.

The lack of significant correlations between turbinal variables corrected by TTSA with elevation (Fig. 5), contrasting with the common expectation, suggests that respiratory turbinal proportions do not directly adapt to elevation in Thomasomys. Instead, our findings align with the idea that other high-elevation adaptations such as breathing rate may also play an important role rather than turbinal morphology alone (Storz et al. 2010; Ivy and Scott 2015; Withers et al. 2016b).

Furthermore, other environmental factors such as temperature or humidity could also be driving the evolution of turbinal structures (Green et al. 2012; Martinez et al. 2020; Flekkøy et al. 2023), suggesting that turbinal adaptations in Thomasomys are likely to involve both morphological and physiological adaptations to cope with highelevation environments, highlighting the need for a multifactorial approach to understanding nasal adaptations in mammals.

## Response to bioclimatic factors.

The positive and negative correlations observed between turbinal surface areas of Thomasomys and bioclimatic variables highlight the potential adaptive significance of these structures in response to diverse environmental conditions (Tables 1–3; Supplementary Data SD10). Notably, the significant correlation of RTSA—when accounting for TTSA and for phylogeny using RTSA as a function of TTSA—with a wide range of bioclimatic variables (Tables 1 and 3) suggests that Thomasomys species have specific adaptations in response to diverse temperatures and precipitation levels, with a proportional adjustment of respiratory turbinals that may contribute to water balance. This result mirrors findings in some bats and rodents that use their nasal turbinals to minimize water loss in arid environments (Cortés et al. 1990; Nelson et al. 2007; Van Sant et al. 2012). The correlations with precipitation suggest that the Thomasomys species adapt their turbinal structures to manage moisture through efficient air humidification and dehumidification processes in forest habitats that include diverse ecosystems spanning pre-montane, montane, and paramo regions across different phytoregions and ecoregions in the Tropical Andes (Tejedor Garavito et al. 2012; Pacheco 2015; Britto 2017). The diverse climatic conditions influenced by Pacific and Atlantic winds, the rain shadow effect, and atmospheric circulation patterns, create a complex environment (Kattan et al. 2004; Killeen et al. 2007). Precipitation is particularly influential in affecting forest structure, nutrient dynamics, and topography in the Tropical Andes (Clark et al. 2014; Shrestha et al. 2021). This complex interplay of environmental conditions has likely driven the evolution of unique adaptations in Thomasomys species, facilitating their survival in varied Andean forests. Features such as complex scrolling, increased turbinal size, and variations in turbinal proportions at higher elevations and in areas of high precipitation suggest that these adaptations enhance the ability of Thomasomys species to thrive in diverse environments of the Tropical Andes.

On the other hand, the significant correlation between relative RTSA—adjusted by phylogeny using RTSA as a function of SL—and temperature seasonality (Bio 4; Table 2) suggests an adaptation to fluctuating temperatures, which is consistent with findings in other mammals inhabiting arctic and desert habitats, where nasal turbinals play an important role in thermoregulation (Dawson and Schmidt-Nielsen 1966; Van Valkenburgh et al. 2011; Green et al. 2012; Martinez et al. 2024a). In Thomasomys, this adaptation may facilitate efficient heat and moisture conservation in the fluctuating temperatures of montane forests by increasing the RTSA. However, our regression results for the other comparisons with RTSA and OTSA, when sizing by SL, are nonsignificant for the bioclimatic variables (Table 1). Such an absence of correlation does not necessarily indicate that these structures do not have adaptations to cope with their environmental factors. Rather, it suggests that environmental factors other than temperature and precipitation might play a more substantial role in their ecological adaptations. As an example, in canid and arctoid carnivorans, Green et al. (2012) did not find a significant relationship between RTSA and climate as estimated by latitude. This finding suggests that the scaling of respiratory turbinals is not strongly driven by climate-related factors. Instead, other ecological parameters such as diet and habitat appear to have a more significant impact (Green et al. 2012).

The significant correlation found between relative OTSA—when accounting for TTSA and for phylogeny using OTSA as a function of TTSA—and most bioclimatic variables (Tables 1 and 3; Supplementary Data SD10), may reflect the ecological and biological significance of olfactory capabilities in Thomasomys. Olfaction is essential for the survival of most mammals, playing key roles in finding food, identifying mates and offspring, avoiding threats, and marking of territory (e.g. Buck and Axel 1991; Rosell and Sanda 2006; Niimura 2012; Poddar-Sarkar and Brahmachary 2014; McClanahan and Rosell 2020). Beyond allometric scaling, the relative size of olfactory turbinals have been shown to evolve in response to ecological pressures, such as diet, lifestyle, or prey detection (Green et al. 2012; Martinez et al. 2018). This evolution is evident across several mammalian taxa, with ongoing debates about the functional link between the size of olfactory turbinals and correlated olfactory capabilities, such as olfactory sensitivity, particularly in carnivores and insectivores (Green et al. 2012; Martinez et al. 2018, 2023b, 2024c). Even herbivores like rabbits known for their relatively simple diets possess highly sensitive olfaction (Schalken 1976; Schaal et al. 2003). Their unique nose-wiggling behavior enhances their ability to detect chemical molecules and pheromones, which are essential for environmental navigation and mating (Melo and González-Mariscal 2010; Kromin and Ignatova 2014). This functional diversity of olfaction across different mammalian taxa highlights the potential adaptive flexibility of olfactory turbinals in Thomasomys.

Thomasomys species have a diverse array of diets ranging from herbivory to omnivory (López-Arévalo et al. 1993; Pacheco 2015; Sahley et al. 2015). As a result, enhanced olfactory capabilities could be critical for locating food sources in diverse montane forests. Studies based on stomach contents (Noblecilla and Pacheco 2013) and fecal analysis (Sahley et al. 2015) have found dietary variations. Mid-sized species like T. notatus and T. kalinowskii, as well as the larger species like T. aff. aureus, primarily consume seeds (acting as seed dispersers), while smaller species, such as Thomasomys sp. 8 (identified as T. oreas), exhibit more varied or insectivorous diets. The mid-sized species T. laniger has been described as an opportunistic eater, consuming more insects during the rainy season and a diverse array of seeds when fruits are abundant (López-Arévalo et al. 1993). Our findings show that the mid-sized species of the Cinereus and Incanus groups, which likely rely on seed consumption, have a proportionally larger turbinal surface area compared to the larger species T. aureus or T. antoniobracki (Fig. 3; Supplementary Data SD4). The significant correlation between OTSA and most bioclimatic variables (Tables 1 and 3; Supplementary Data SD10) suggests an adaptive response to environmental pressures in montane ecosystems where climatic conditions also influence food availability, although it will be difficult to test due to the lack of ecological data for this genus. Despite this scarcity, discrete observation on the olfactory turbinals of T. pardignasi and T. aureus of the Aureus group lead Brito et al. (2021) to hypothesize that these species are omnivorous, based on the complex olfactory turbinals (found to be related to earthworm consumption; Martinez et al. 2018) and their hypsodont teeth, which could be a response to an herbivorous diet. However, further quantitative research such as stomach content analysis or metabarcoding is required to fully validate the link between olfactory turbinals and diet in these rodents.

Overall, these findings align with the broader concept that turbinals are multifunctional structures in mammals, evolving under a suite of environmental pressures (Jackson and Schmidt-Nielsen 1964; Green et al. 2012; Martinez et al. 2024a). In Thomasomys, the complexity of these adaptations likely reflects the unique ecological challenges of their montane environments in the Andes. Although this study does not include Thomasomys species living at the highest elevations such as T. silvestris (1,800 to 4,500 m) and T. vulcani (1,400 to 4,500m) belonging to the Cinereus group, both of which thrive in paramo and high montane forests, these species likely exhibit similar adaptations to counterparts of this group analyzed here. The capacity of Thomasomys to occupy a wide altitudinal range reinforces their specialization in coping with the environmental challenges in these

#### The interdependence of respiratory and olfactory turbinals.

This study primarily emphasizes the respiratory turbinals of Thomasomys as a proxy of heat and moisture conservation; however, olfactory turbinals also provide valuable insights into their potential olfactory capabilities. The positive correlation between the RTSA and OTSA and between the naso- and maxilloturbinals (Fig. 4) may carry potential biological implications, hinting at possible co-dependence in response to certain environmental or physiological demands. These findings contrast with the traditionally observed evolutionary tradeoffs between these structures in various mammalian groups (e.g., Van Valkenburgh et al. 2011; Green et al. 2012; Martinez et al. 2018, 2020, 2024a), where the development of one set of turbinals often comes at the expense of the other. The absence of such a trade-off in Thomasomys implies greater developmental flexibility, allowing simultaneous optimization of both respiration and olfaction. This flexibility may facilitate the ability of Thomasomys to adapt to a range of selective pressures such as the need for efficient respiration at high elevations or enhanced olfactory capabilities, potentially contributing to their success in the montane forests.

Furthermore, our findings—possibly influenced by focusing on closely-related species from the same genus—indicate that evolutionary trade-offs in turbinal morphology may vary across different taxonomic categories as has been found in other studies (e.g., Green et al. 2012; Martinez et al. 2018, 2024a, 2024b). The diversity in turbinal surface area observed along elevational gradients could be related to the speciation process in Thomasomys, likely driven by the varying habitats and environmental conditions at different elevations. For example, species at higher elevations may experience distinct obstacles concerning heat and moisture conservation compared to those in lower, more humid locations, thereby influencing the evolution of their turbinal structures (Marks et al. 2019; Martinez et al. 2020, 2024a).

This interdependence may reflect broader evolutionary adaptations in Thomasomys, where the ability to optimize both respiratory and olfactory functions offers an adaptive advantage in diverse Andean environments. Further research, such as examining sensory ecology alongside respiratory physiology, could provide further information about how these interrelated traits have shaped evolutionary pathways in the genus.

## Other factors influencing the evolution of turbinals.

Our findings reveal that, in general, medium- and large-seized Thomasomys species have larger respiratory turbinal surface area relative to their skull size compared to their counterparts (positive allometry, S=2.92, Fig. 3D). This trend aligns with previous studies in murine rodents as well as on the scale of small non-flying mammals and Carnivora, where the correlation between the respiratory turbinals and SL shows positive allometry (S = 2.21, 2.49, and 2.27, respectively; Green et al. 2012; Martinez et al. 2018, 2020). Similarly, the correlation between the maxilloturbinal and SL on the scale of mammals also shows positive allometry (S=2.60; Martinez et al. 2024a). However, deviations from this trend were noted in larger Thomasomys species, such as those of the Aureus group, which tend to have relatively reduced respiratory surface area relative to their skull size compared to their counterparts (Fig. 3D; Supplementary Data 7). This finding suggests that increasing body size may be associated with a relative reduction in respiratory turbinal surface area. Such reductions could reflect functional adaptations because larger-bodied animals often exhibit lower mass-specific metabolic rates (Harrison 2018). Green et al. (2012) found an isometric relationship between the surface area of respiratory turbinals and the volume of the nasal chamber, suggesting that larger caniform species tend to have relatively less respiratory surface area compared to the volume of their nasal chamber. This reduction was interpreted as an adaptation to reduce heat loss in larger species because their larger body size naturally provides greater thermal stability (Green et al. 2012). Overall, this pattern highlights that results may vary using different size proxies, ecological factors, and taxonomic groups when interpreting these morphological traits.

The ethmoturbinals (= olfactory turbinals) hold significant taxonomic relevance as noted by Pacheco (2015), Pacheco and Ruelas (2023), and Brito et al. (2021), who observed distinct variations in their relative sizes across different species. These authors noted that midsized species, such as T. caudivarius, T. incanus, T. ischyrus, and T. kalinowskii, along with the smaller species T. taczanowskii exhibit larger olfactory turbinals. In contrast, the large-sized species T. aureus and mid-sized species, such as T. auricularis, T. cinereus, T. lojapiuranus, T. notatus, and T. shallqukucha tend to have moderately sized olfactory turbinals. Meanwhile, mid-sized species including T. pagaibambensis, T. pardignasi, and T. pyrrhonotus stand out with smaller and less developed turbinals. These observations, primarily based on external examinations, underline the potential of ethmoturbinals as a taxonomic tool. However, our quantitative data show that small-sized species tend to have smaller turbinals (e.g., T. taczanowskii, T. daphne), while mid- and large-sized species have larger turbinals (e.g., T. pagaibambensis, T. ischyrus; Fig. 3A-C). These findings contrast with earlier observations that T. taczanowskii has larger turbinals and that midsized species of the Cinereus group has moderately- or smaller-sized turbinals compared to its counterparts. To resolve these discrepancies, it will be necessary to increase sample sizes of specimens and species for a more comprehensive analysis.

Additionally, some species groups showed different trends in our analysis. For instance, species of the Aureus E, Aureus W, Incanus, and mid-sized species of the Cinereus groups displayed noticeably slight increase or decrease trends in some analyses, while in the remaining groups no trend was noticed. This remark is significant because it is possible that some of these trends are associated with phylogenetic inertia, though it is crucial to increase sampling for confirmation. Of the 53 valid species (Brito et al. 2024), we have data for only 10 (including Thomasomys cf. dispar). The 9 remaining species used here are candidates proposed by Pacheco (2003; 2015) and Ruelas et al. (2024), and not all have molecular data available. Previous studies in other mammals have found a significant phylogenetic signal related to turbinal variation (e.g., Green et al. 2012; Martinez et al. 2018, 2020, 2024a). Our phylogenetic scaling analysis suggested that RTSA and OTSA as a function of SL are influenced by evolutionary history (Grafen model) and gradual evolution (Brownian motion), respectively. In contrast, RTSA and OTSA—when analyzing as function of TTSA—are influenced primarily by direct morphological scaling, suggesting a different evolutionary dynamic. These findings point to the need for a more comprehensive sampling to fully explore the taxonomic and evolutionary significance of turbinal variations in the Thomasomys species.

Our study included a significant representation of the small-sized and widely distributed species T. taczanowskii, ranging from 1,500 to 2,950 m in elevation (Appendix I). Notably, the turbinal surface areas (both respiratory and olfactory) of T. taczanowskii showed relative consistency across all elevations, with no apparent pattern in any of

the variables analyzed (Fig 5). Additionally, we observed size and turbinal surface area variations between 2 adult specimens of the midsized T. notatus, aged ~3 and 5 (following Pacheco and Ruelas 2023). Typically, taxonomic studies focus on ages 3 and 4 because older specimens can have flatter and broader skulls, which might affect statistical analyses (Ruelas D, [UNMSM, Lima, Peru], personal observation, [06 July 2025]). Our observations suggest that in Thomasomys, age may significantly influence morphological characteristics, with younger specimens having smaller turbinals than those in the older specimens. Despite being based on only 2 specimens, these findings align with other studies (Mason et al. 2020; Ito et al. 2022), showing turbinal size and complexity differences between juvenile and adult stages in some species.

We previously hypothesized that turbinals of Thomasomys might reflect adaptations to live in high-elevation environments. Given the likely Amazonian origin of the Thomasomyini tribe—which includes Tropical Andes specialist genera, including Aepeomys, Chilomys, and Thomasomys, along with the widely distributed Rhipidomys—and their subsequent migration into the Andes (Schenk and Steppan 2018), ancestral forms may have had smaller, less-developed turbinals. Scans from Brito et al. (2022) showed that Andean thomasomyines such as C. instans and C. georgeledecii (ranging from 1,502 to 2,350 m), have less scrolled and simpler turbinals compared to C. neisi (ranging from 2,500 to 2,900 m) and C. percequilloi (ranging from 1,090 to 3,400 m). In contrast, turbinals in the lowland species R. leucodactylus (FMNH 68654) were observed to be less developed and less scrolled than those seen in Thomasomys (Ruelas D, [UNMSM, Lima, Peru], personal observation, [06 July 2025]; also see Pacheco 2003). This finding suggests a significant evolutionary adaptation to high-elevation environments such as montane forests, leading to their successful radiation in these challenging habitats. To substantiate this hypothesis, comprehensive molecular studies involving multiple genetic loci are necessary. Furthermore, examining adaptations in other high-elevation rodents like the deer mouse Peromyscus maniculatus (Snyder 1982; Storz et al., 2007, 2010), provides valuable comparisons for understanding potential genetic adaptations in Thomasomys. This broader perspective will enhance our understanding of the evolutionary and ecological significance of respiratory turbinals in adapting Thomasomys to diverse environmental conditions.

Furthermore, future research should also explore other adaptive factors such as epithelium thickness, venous system expansion, and specialized aquaporin distributions in turbinals hypothesized to be involved in high-elevation habitat adaptation (Gallardo et al. 2008; Smith et al. 2022). The relationship between bony respiratory turbinals and physiological traits like basal metabolic rate or body temperature remains unclear (Martinez et al. 2024a, b), and addressing this gap is important to fully understand the scope of turbinal adaptations. Cellular-level research using histology and diceCT techniques to identify specific alterations associated with the venous system, mucus glands, or ciliated structures will provide deeper insight into the physiological changes in high-elevation species.

# Acknowledgments

We thank Elizabeth Escobar, Diego Marcelo, Maria Peralta, Carlos Jiménez, Edith Salas, Mariela Leo, Jessica Amanzo, Marina Villalobos, and other colleagues for collecting the specimens used here. We thank Anthony Pauca for software support in obtaining Bioclim variables and Omar Ruelas for assistance with the "ggplot2" package. We also thank Adam Ferguson (Field Museum of Natural History, Chicago) for lending us some specimens. We thank Renaud Lebrun and Arthur Naas for their help with the CT facilities. CT data acquisitions were performed using the micro-computed tomography (µCT) facilities of the MRI platform member of the national infrastructure France-BioImaging supported by the French National Research Agency (Grant ANR-10-INBS-04, "Investments for the future") and those of the Laboratoire d'Excellence Centre Méditerranéen de l'Environnement et de la Biodiversité (LabEx CeMEB, ANR10-LABX-0004). This is a contribution of ISEM 2025-X, Univ Montpellier, CNRS, EPHE, IRD, Montpellier, France.

#### **Author contributions**

Dennisse Ruelas (Conceptualization, Data curation, Formal analysis, Investigation, Methodology, Visualization, Writing—original draft, Writing—review & editing), Pierre-Henri Fabre (Conceptualization, Funding acquisition, Methodology, Supervision, Validation, Visualization, Writing—review & editing), Victor Pacheco (Data curation, Supervision, Validation, Writing—review & editing), and Quentin Martinez (Conceptualization, Methodology, Supervision, Validation, Visualization, Writing—review & editing)

# Supplementary data

Supplementary data are available at Journal of Mammalogy online.

## **Funding**

Funding was provided by the Agence Nationale de la Recherche (Défi des autres savoirs, Grants DS10, ANR-17-CE02-0005 RHINOGRAD 2017, P.H.F.). This work was supported by CONCYTEC through the PROCIEN-CIA program within the framework of the "Basic Research Projects" contest 2022-01, according to contract No. PE501078825-2022- PRO-CIENCIA. D.R. was supported by a scholarship of the Franco Peruvian School of Life Sciences. This is a contribution of ISEM 2025-159 SUD, Univ Montpellier, CNRS, EPHE, IRD, Montpellier, France. The authors thank the Bundesministerium für Bildung und Forschung (BMBF; Project KI-Morph 05D2022).

Conflict of interest statement None declared.

## **Data Availability**

Data used in analyses are presented in Supplementary Data SD4.

#### References

- Apfelbach R, Blanchard CD, Blanchard RJ, Hayes RA, McGregor IS. 2005. The effects of predator odors in mammalian prey species: a review of field and laboratory studies. Neuroscience & Biobehavioral Reviews 29(8):1123-1144. https://doi.org/10.1016/j.neubiorev.2005.05.005
- Arias-Reyes C, Soliz J, Joseph V. 2021. Mice and rats display different ventilatory, hematological, and metabolic features of acclimatization to hypoxia. Frontiers in Physiology 12:647822. https://doi.org/10.3389/ fphys.2021.647822
- Barrios AW, Núñez G, Sánchez Quinteiro P, Salazar I. 2014. Anatomy, histochemistry, and immunohistochemistry of the olfactory subsystems in mice. Frontiers in Neuroanatomy 8:63. https://doi.org/ 10.3389/fnana.2014.00063
- Barton RA. 2006. Olfactory evolution and behavioral ecology in primates. American Journal of Primatology 68(6):545-558. https://doi.org/ 10.1002/ajp.20251
- Bolboacă SD, Jäntschi I. 2006. Pearson versus Spearman, Kendall's tau correlation analysis on structure-activity relationships of biologic active compounds. Leonardo Journal of Sciences 5(9):179-200.
- Bowlby HD, Gibson AJF. 2015. Environmental effects on survival rates: robust regression, recovery planning and endangered Atlantic

- salmon. Ecology and Evolution 5(16):3450-3461. https://doi.org/ 10.1002/ece3.1614
- Brandão MV, Percequillo AR, D'Elía G, Paresque R, Carmignotto AP. 2021. A new species of Akodon Meyen, 1833 (Rodentia: Cricetidae: Sigmodontinae) endemic from the Brazilian Cerrado. Journal of Mammalogy 102(1):101–122. https://doi.org/10.1093/jmammal/gyaa126
- Brito J, García R, Castellanos FX, Gavilanes G, Curay J, Carrión-Olmedo JC, Reves-Barriga D, Guayasamin JM, Salazar-Bravo J, Pinto CM. 2024. Two new species of Thomasomys (Cricetidae: Sigmodontinae) from the western Andes of Ecuador and an updated phylogenetic hypothesis for the genus. Vertebrate Zoology 74:709–734. https://doi.org/10. 3897/vz.74.e128528
- Brito J, Vaca-Puente S, Koch C, Tinoco N. 2021. Discovery of the first Amazonian Thomasomys (Rodentia, Cricetidae, Sigmodontinae): a new species from the remote Cordilleras del Cóndor and Kutukú in Ecuador. Journal of Mammalogy 102(2):615-635. https://doi.org/10.1093/ jmammal/gyaa183
- Brito MJ, Teska WR, Ojala-Barbour R. 2012. Descripción del nido de dos especies de Thomasomys (Cricetidae) en un bosque alto-andino en Ecuador. Therya 3(2):263-268. https://doi.org/10.12933/therya-12-71
- Britto B. 2017. Update of the terrestrial ecoregions of Peru proposed in the Red book of endemic plants of Peru. Gayana. Botánica 74(ahead):0-29. https://doi.org/10.4067/S0717-66432017005000318
- Buck L, Axel R. 1991. A novel multigene family may encode odorant receptors: a molecular basis for odor recognition. Cell 65(1):175-187. https://doi.org/10.1016/0092-8674(91)90418-x
- Burnham KP, Anderson DR. 2004. Multimodel inference: understanding AIC and BIC in model selection. Sociological Methods & Research 33(2):261–304. https://doi.org/10.1177/0049124104268644
- Butaric LN, Klocke RP. 2018. Nasal variation in relation to high-altitude adaptations among Tibetans and Andeans. American Journal of Human Biology 30(3):e23104. https://doi.org/10.1002/ajhb.23104
- Butler MA, King AA. 2004. Phylogenetic comparative analysis: a modeling approach for adaptive evolution. The American Naturalist 164(6):683-695. https://doi.org/10.1086/426002
- Caputa M. 1979. Temperature gradients in the nasal cavity of the rabbit. Journal of Thermal Biology 4(4):283-286. https://doi.org/10.1016/ 0306-4565(79)90016-0
- Clark KE, Torres MA, West AJ, Hilton RG, New M, Horwath AB, Fisher JB, Rapp JM, Robles Caceres A, Malhi Y. 2014. The hydrological regime of a forested tropical Andean catchment. Hydrology and Earth System Sciences 18(12):5377-5397. https://doi.org/10.5194/hess-18-5377-2014
- Cortés A, Rosenmann M, Baez C. 1990. Función del riñón y del pasaje nasal en la conservación de agua corporal en roedores simpátridos de Chile central. Revista Chilena de Historia Natural 63:279-291.
- Cortés A, Tirado C, Rosenmann M. 2003. Energy metabolism and thermoregulation in Chinchilla brevicaudata. Journal of Thermal Biology 28(6-7):489-495. https://doi.org/10.1016/S0306-4565(03)00049-4
- Dawson T, Schmidt-Nielsen K. 1966. Effect of thermal conductance on water economy in the antelope jack rabbit, Lepus alleni. Journal of Cellular Physiology 67(3):463-471. https://doi.org/10.1002/jcp.1040670311
- Felsenstein J. 1985. Phylogenies and the comparative method. The American Naturalist 125(1):1-15.
- Fick SE, Hijmans RJ. 2017. WorldClim 2: new 1-km spatial resolution climate surfaces for global land areas. International Journal of Climatology 37(12):4302-4315. https://doi.org/10.1002/joc.5086
- Flekkøy EG, Folkow LP, Kjelstrup S, Mason MJ, Wilhelmsen Ø. 2023. Thermal modeling of the respiratory turbinates in arctic and subtropical seals. Journal of Thermal Biology 112:103402. https://doi.org/10.1016/j. jtherbio.2022.103402
- Freckleton PR, Harvey HP, Pagel M. 2002. Phylogenetic analysis and comparative data: a test and review of evidence. The American Naturalist 160(6):712-726. https://doi.org/10.1086/343873

- Gallardo P, Herrera S, Saffer K, Bozinovic F. 2008. Distribución de acuaporinas en los pasajes nasales de Octodon degus, un roedor de ambientes desérticos sudamericanos: implicaciones en la conservación de agua. Revista Chilena de Historia Natural 81(1):33-40. https://doi. org/10.4067/S0716-078X2008000100003
- Ghent AW. 1963. Kendall's "Tau" coefficient as an index of similarity in comparisons of plant or animal communities. The Canadian Entomologist 95(6):568-575. https://doi.org/10.4039/Ent95568-6
- Grafen A. 1989. The phylogenetic regression. Philosophical Transactions of the Royal Society of London. Series B, Biological Sciences 326(1233):119–157. https://doi.org/10.1098/rstb.1989.0106
- Green PA, Van Valkenburgh B, Pang B, Bird D, Rowe T, Curtis A. 2012. Respiratory and olfactory turbinal size in canid and arctoid carnivorans. Journal of Anatomy 221(6):609-621. https://doi.org/10.1111/ j.1469-7580.2012.01570.x
- Harkema JR, Carey SA, Wagner JG. 2006. The nose revisited: a brief review of the comparative structure, function, and toxicologic pathology of the nasal epithelium. Toxicologic Pathology 34(3):252-269. https:// doi.org/10.1080/01926230600713475
- Harrison JF. 2018. Approaches for testing hypotheses for the hypometric scaling of aerobic metabolic rate in animals. American Journal of Physiology-Regulatory, Integrative and Comparative Physiology 315(5):R879–R894. https://doi.org/10.1152/ajpregu.00165.2018
- Hillenius WJ. 1992. The evolution of nasal turbinates and mammalian endothermy. Paleobiology 18(1):17-29. https://doi.org/10.1017/ S0094837300012197
- Hothorn T, Bretz F, Westfall P, Heiberger RM, Schuetzenmeister A, Scheibe S 2024. multcomp: Simultaneous Inference in General Parametric Models. https://cran.r-project.org/web/packages/multcomp/index.
- Hurtado N, D'Elía G. 2022. Historical biogeography of a rapid and geographically wide diversification in Neotropical mammals. Journal of Biogeography 49(5):781-793. https://doi.org/10.1111/jbi.14352
- Ito K, Kodeara R, Koyasu K, Martinez Q, Koyabu D. 2022. The development of nasal turbinal morphology of moles and shrews. Vertebrate Zoology 72:857-881. https://doi.org/10.3897/vz.72.e85466
- Ivy CM, Scott GR. 2015. Control of breathing and the circulation in high-altitude mammals and birds. Comparative Biochemistry and Physiology Part A: Molecular & Integrative Physiology 186:66-74. https://doi.org/10.1016/j.cbpa.2014.10.009
- Jackson DC, Schmidt-Nielsen K. 1964. Countercurrent heat exchange in the respiratory passages. Proceedings of the National Academy of Sciences of the United States of America 51(6):1192-1197. https:// doi.org/10.1073%2Fpnas.51.6.1192
- Jarantow SW, Pisors ED, Chiu ML. 2023. Introduction to the use of linear and nonlinear regression analysis in quantitative biological assays. Current Protocols 3(6):e801. https://doi.org/10.1002/cpz1.801
- Kattan GH, Franco P, Rojas V, Morales G. 2004. Biological diversification in a complex region: a spatial analysis of faunistic diversity and biogeography of the Andes of Colombia. Journal of Biogeography 31(11):1829-1839. https://doi.org/10.1111/j.1365-2699.2004.01109.x
- Killeen TJ, Douglas M, Consiglio T, Jørgensen PM, Mejia J. 2007. Dry spots and wet spots in the Andean hotspot. Journal of Biogeography 34(8):1357–1373. https://doi.org/10.1111/j.1365-2699.2006.01682.x
- Koller M, Stahel WA. 2011. Sharpening Wald-type inference in robust regression for small samples. Computational Statistics & Data Analysis 55(8):2504-2515. https://doi.org/10.1016/j.csda.2011.02.014
- Kromin AA, Ignatova Y. 2014. Objective method for registration of the sniffing component of the search behavior in rabbits subjected to food deprivation. Bulletin of Experimental Biology and Medicine 156(4):522-525. https://doi.org/10.1007/s10517-014-2389-0
- Leo LM, Gardner AL. 1993. A new species of a giant Thomasomys (Mammalia: Muridae: Sigmodontinae) from the Andes of northcentral

- Peru. Proceedings of the Biological Society of Washington 106(3):417-428.
- Llerena-Zambrano M, Ordoñez JC, Llambí LD, Van Der Sande M, Pinto E, Salazar L, Cuesta F. 2021. Minimum temperature drives community leaf trait variation in secondary montane forests along a 3000-m elevation gradient in the tropical Andes. Plant Ecology & Diversity 14(1-2):47-63. https://doi.org/10.1080/17550874.2021.1903604
- López-Arévalo H, Montenegro O, Cadena A. 1993. Ecología de los pequeños mamíferos de la reserva biológica carpanta, en la cordillera oriental Colombiana. Studies on Neotropical Fauna and Environment 28(4):193-210. https://doi.org/10.1080/01650529309360904
- Lourenço VM, Pires AM, Kirst M. 2011. Robust linear regression methods in association studies. Bioinformatics 27(6):815-821. https://doi. org/10.1093/bioinformatics/btr006
- Lui MA, Mahalingam S, Patel P, Connaty AD, Ivy CM, Cheviron ZA, Storz JF, McClelland GB, Scott GR. 2015. High-altitude ancestry and hypoxia acclimation have distinct effects on exercise capacity and muscle phenotype in deer mice. American Journal of Physiology—Regulatory, Integrative and Comparative Physiology 308(9):R779-R791. https:// doi.org/10.1152/ajpregu.00362.2014
- Luna F, Naya H, Naya DE. 2017. Understanding evolutionary variation in basal metabolic rate: an analysis in subterranean rodents. Comparative Biochemistry and Physiology Part A: Molecular & Integrative Physiology 206:87–94. https://doi.org/10.1016/j.cbpa.2017.02.002
- Maechler M, Rousseeuw P, Croux C, Todorov V, Ruckstuhl A, Salibian-Barrera M, Verbeke T, Koller M, Conceicao ELT, di Palma MA. 2024. robustbase: Basic Robust Statistics. https://cran.r-project.org/web/ packages/robustbase/index.html
- Marks TN, Maddux SD, Butaric LN, Franciscus RG. 2019. Climatic adaptation in human inferior nasal turbinate morphology: evidence from Arctic and equatorial populations. American Journal of Physical Anthropology 169(3):498–512. https://doi.org/10.1002/ajpa.23840
- Martinez Q, Amson E, Ruf I, Smith TD, Pirot N, Broyon M, Lebrun R, Captier G, Gascó Martín C, Ferreira G, et al. 2024a. Turbinal bones are still one of the last frontiers of the tetrapod skull: hypotheses, challenges and perspectives. Biological Reviews 99(6):2304-2337. https://doi. org/10.1111/brv.13122
- Martinez Q, Amson E, Laska M. 2024c. Does the number of functional olfactory receptor genes predict olfactory sensitivity and discrimination performance in mammals? Journal of Evolutionary Biology 37(2):238–247. https://doi.org/10.1093/jeb/voae006
- Martinez Q, Clavel J, Esselstyn JA, Achmadi AS, Grohé C, Pirot N, Fabre P-H. 2020. Convergent evolution of olfactory and thermoregulatory capacities in small amphibious mammals. Proceedings of the National Academy of Sciences 117(16):8958-8965. https://doi.org/ 10.1073/pnas.1917836117
- Martinez Q, Courcelle M, Douzery E, Fabre P-H. 2023b. When morphology does not fit the genomes: the case of rodent olfaction. Biology Letters 19(4):20230080. https://doi.org/10.1098/rsbl.2023.0080
- Martinez Q, Lebrun R, Achmadi AS, Esselstyn JA, Evans AR, Heaney LR, Miguez RP, Rowe KC, Fabre P-H. 2018. Convergent evolution of an extreme dietary specialisation, the olfactory system of worm-eating rodents. Scientific Reports 8(1):17806. https://doi.org/10.1038/s41598-018-35827-0
- Martinez Q, Okrouhlík J, Šumbera R, Wright M, Araújo R, Braude S, Hildebrandt TB, Holtze S, Ruf I, Fabre P-H. 2023a. Mammalian maxilloturbinal evolution does not reflect thermal biology. Nature Communications 14(1):4425. https://doi.org/10.1038/s41467-023-39994-1
- Martinez Q, Wright M, Dubourguier B, Ito K, van de Kamp T, Hamann E, Zuber M, Ferreira G, Blanc R, Fabre P-H, et al. 2024b. Disparity of turbinal bones in placental mammals. The Anatomical Record 1–29 https://doi.org/10.1002/ar.25552

- Martins EP, Hansen TF. 1997. Phylogenies and the comparative method: a general approach to incorporating phylogenetic information into the analysis of interspecific data. The American Naturalist 149(4):646-667. https://doi.org/10.1086/286013
- Mason MJ, Wenger LMD, Hammer Ø, Blix AS. 2020. Structure and function of respiratory turbinates in phocid seals. Polar Biology 43(2):157–173. https://doi.org/10.1007/s00300-019-02618-w
- McClanahan K, Rosell F. 2020. Conspecific recognition of pedal scent in domestic dogs. Scientific Reports 10(1):17837. https://doi.org/10.1038/ s41598-020-74784-5
- Melo AI, González-Mariscal G. 2010. Communication by olfactory signals in rabbits: its role in reproduction. Vitamins and Hormones 83:351-371. https://doi.org/10.1016/S0083-6729(10)83015-8
- Min SH, Zhou J. 2021. smplot: an R package for easy and elegant data visualization. Frontiers in Genetics 12:802894-802810.
- Mitchell DR, Sherratt E, Weisbecker V. 2024. Facing the facts: adaptive trade-offs along body size ranges determine mammalian craniofacial scaling. Biological Reviews 99(2):496–524. https://doi.org/10.1111/
- Monge C, Leon-Velarde F. 1991. Physiological adaptation to high altitude: oxygen transport in mammals and birds. Physiological Reviews 71(4):1135–1172. https://doi.org/10.1152/physrev.1991.71.4.1135
- Moulton DG. 1967. Olfaction in mammals. American Zoologist 7(3):421– 429. https://doi.org/10.1093/icb/7.3.421
- Nelson JE, Christian KA, Baudinette RV. 2007. Anatomy of the nasal passages of three species of Australian bats in relation to water loss. Australian Journal of Zoology 55(1):57-62. https://doi.org/10.1071/ ZO06101
- Niimura Y. 2012. Olfactory receptor multigene family in vertebrates: from the viewpoint of evolutionary genomics. Current Genomics 13(2):103-114. https://doi.org/10.2174/138920212799860706
- Noblecilla MC, Pacheco V. 2013. Dieta de roedores sigmodontinos (Cricetidae) en los bosques montanos tropicales de Huánuco, Perú. Revista Peruana de Biología 19(3):317-322. https://doi.org/10.15381/rpb. v19i3.1046
- Ooms J, McNamara J. 2024. Writexl: Export data frames to excel "xlsx" Format. https://cran.r-project.org/web/packages/writexl/index.html
- Pacheco V. 2003. Phylogenetic analyses of the Thomasomyini (Muroidea: Sigmodontinae) based on morphological data. Ph.D. dissertation. The City University of New York, New York.
- Pacheco V. 2015. Genus Thomasomys Coues, 1884. In: Mammals of South America. Volume 2, Rodents. Chicago: The University of Chicago Press; p. 617-682
- Pacheco V, Patton JL, D'Elía G. 2015. Tribe Thomasomyini Steadman and Ray, 1982. In: Mammals of South america. Volume 2, Rodents. Chicago (IL, USA): The University of Chicago Press; p. 571-574
- Pacheco V, Ruelas D. 2023. Systematic revision of Thomasomys cinereus (Rodentia: Cricetidae: Sigmodontinae) from northern Peru and southern Ecuador, with descriptions of three new species. Bulletin of the American Museum of Natural History 461(1):71.
- Pang B, Yee KK, Lischka FW, Rawson NE, Haskins ME, Wysocki CJ, Craven BA, Van Valkenburgh B. 2016. The influence of nasal airflow on respiratory and olfactory epithelial distribution in felids. The Journal of Experimental Biology 219(Pt 12):1866–1874. https://doi.org/10.1242/ jeb.131482
- Parada A, D'Elía G, Palma RE. 2015. The influence of ecological and geographical context in the radiation of Neotropical sigmodontine rodents. BMC Evolutionary Biology 15(1). https://doi.org/10.1186/ s12862-015-0440-z
- Paradis E, Schliep K. 2019. ape 5.0: an environment for modern phylogenetics and evolutionary analyses in R. Bioinformatics 35(3):526-528.
- Pardiñas UFJ, Teta P, Alvarado-Serrano D, Geise L, Jayat JP, Ortiz PE, Gonçalves PR, D'Elía G. 2015. Genus Akodon Meyen, 1833. In:

- Mammals of South America. Volume 2, Rodents. Chicago (IL, USA): The University of Chicago Press; p. 144-204.
- Parsons TS. 1967. Evolution of the nasal structure in the lower tetrapods. American Zoologist 7(3):397–413. https://doi.org/10.1093/icb/7.3.397
- Patterson BD, Solari S, Velazco PM. 2012. The role of the Andes in the diversification and biogeography of Neotropical mammals. In: Bones, clones, and biomes. Chicago (IL, USA): The University of Chicago Press; p. 351-378.
- Pinheiro J, Bates D, DebRoy S, Sarkar D, EISPACK authors Heisterkamp S, Van Willigen B, Ranke J, R Core Team. 2024. nlme: Linear and Nonlinear Mixed Effects Models. https://cran.r-project.org/web/packages/ nlme/index.html
- Poddar-Sarkar M, Brahmachary RL. 2014. Pheromones of Tiger and Other Big Cats. In: Neurobiology of chemical communication. Boca Raton (FL, USA): CRC Press/Taylor & Francis.
- Porto A, Shirai LT, de Oliveira FB, Marroig G. 2013. Size variation, growth strategies, and the evolution of modularity in the mammalian skull. Evolution 67(11):3305–3322. https://doi.org/10.1111/evo.12177
- R Core Team. 2022. R: a language and environment for statistical computing. https://www.R-project.org/
- Revell LJ. 2012. phytools: an R package for phylogenetic comparative biology (and other things): phytools: R package. Methods in Ecology and Evolution 3(2):217-223. https://doi.org/10.1111/j.2041-210X.
- Rezende EL, Gomes FR, Ghalambor CK, Russell GA, Chappelll MA. 2005. An evolutionary frame of work to study physiological adaptation to high altitudes. Revista Chilena de Historia Natural 78(2):323-336. https://doi.org/10.4067/S0716-078X2005000200016
- Rosell F, Sanda J. 2006. Potential risks of olfactory signaling: the effect of predators on scent marking by beavers. Behavioral Ecology 17(6):897-904. https://doi.org/10.1093/beheco/arl022
- RStudio Team. 2024. RStudio: Integrated Development Environment for R. www.rstudio.com/
- Ruelas D, Pacheco V, Pérez J, Diaz-Nieto J, Fabre P-H. 2024. Unilocus delimitation methods reveal the underestimated species diversity of Thomasomys (Rodentia, Cricetidae). Zoologica Scripta 53(6):763-788. https://doi.org/10.1111/zsc.12680
- Ruf I. 2020. Ontogenetic transformations of the ethmoidal region in Muroidea (Rodentia, Mammalia): new insights from perinatal stages. Vertebrate Zoology 70:383-415. https://doi.org/10.26049/VZ70-3-2020-10
- Sahley CT, Cervantes K, Pacheco V, Salas E, Paredes D, Alonso A. 2015. Diet of a sigmodontine rodent assemblage in a Peruvian montane forest. Journal of Mammalogy 96(5):1071-1080. https://doi.org/ 10.1093/jmammal/gyv112
- Schaal B, Coureaud G, Langlois D, Giniès C, Sémon E, Perrier G. 2003. Chemical and behavioural characterization of the rabbit mammary pheromone. Nature 424(6944):68-72. https://doi.org/10.1038/ nature01739
- Schalken APM. 1976. Three types of pheromones in the domestic rabbit, Oryctolagus cuniculus (L). Chemical Senses 2(2):139-155. https://doi. org/10.1093/chemse/2.2.139
- Schenk JJ, Steppan SJ. 2018. The role of geography in adaptive radiation. The American Naturalist 192(4):415–431. https://doi.org/10.1086/699221
- Schippers M-P, Ramirez O, Arana M, Pinedo-Bernal P, McClelland GB. 2012. Increase in carbohydrate utilization in high-altitude Andean mice. Current Biology 22(24):2350-2354. https://doi.org/10.1016/j. cub.2012.10.043
- Schmidt-Nielsen K, Hainsworth FR, Murrish DE. 1970. Counter-current heat exchange in the respiratory passages: effect on water and heat balance. Respiration Physiology 9(2):263-276. https://doi.org/10. 1016/0034-5687(70)90075-7
- Shrestha D, Sharma S, Talchabhadel R, Deshar R, Hamal K, Khadka N, Nakamura K. 2021. Detection of spatial rainfall variation over the

- Andean region demonstrated by satellite-based observations. Atmosphere 12(9):1204. https://doi.org/10.3390/atmos12091204
- Smith TD, Bhatnagar KP. 2004. Microsmatic primates: Reconsidering how and when size matters. The Anatomical Record Part B: The New Anatomist 279(1):24-31. https://doi.org/10.1002/ar.b.20026
- Smith TD, Bhatnagar KP, Rossie JB, Docherty BA, Burrows AM, Cooper GM, Mooney MP, Siegel MI. 2007. Scaling of the first ethmoturbinal in nocturnal strepsirrhines: olfactory and respiratory surfaces. The Anatomical Record 290(3):215-237. https://doi.org/10.1002/ar.20428
- Smith TD, Bonar CJ. 2022. The nasal cavity in agoutis (Dasyprocta spp.): a micro-computed tomographic and histological study. Vertebrate Zoology 72:95-113. https://doi.org/10.3897/vz.72.e76047
- Smith TD, DeLeon VB, Eiting TP, Corbin HM, Bhatnagar KP, Santana SE. 2022. Venous networks in the upper airways of bats: a histological and diceCT study. The Anatomical Record 305(8):1871-1891. https:// doi.org/10.1002/ar.24762
- Smith TD, Eiting TP, Bhatnagar KP. 2012. A quantitative study of olfactory, non-olfactory, and vomeronasal epithelia in the nasal fossa of the bat Megaderma lyra. Journal of Mammalian Evolution 19(1):27–41. https://doi.org/10.1007/s10914-011-9178-6
- Smith TD, Rossie JB. 2008. Nasal fossa of mouse and dwarf lemurs (Primates, Cheirogaleidae). The Anatomical Record: Advances in Integrative Anatomy and Evolutionary Biology 291(8):895-915. https:// doi.org/10.1002/ar.20724
- Spence AR, Tingley MW. 2020. The challenge of novel abiotic conditions for species undergoing climate-induced range shifts. Ecography 43(11):1571–1590. https://doi.org/10.1111/ecog.05170
- Storz JF, Runck AM, Moriyama H, Weber RE, Fago A. 2010. Genetic differences in hemoglobin function between highland and lowland deer mice. The Journal of Experimental Biology 213(Pt 15):2565-2574. https://doi.org/10.1242/jeb.042598
- Storz JF, Sabatino SJ, Hoffmann FG, Gering EJ, Moriyama H, Ferrand N, Monteiro B, Nachman MW. 2007. The Molecular Basis of High-Altitude Adaptation in Deer Mice. PLoS Genetics 3(3):e45. https://doi. org/10.1371/journal.pgen.0030045
- Tejedor Garavito N, Álvarez E, Caro SA, Murakami AA, Blundo C, Espinoza TEB, Cuadros MALT, Gaviria J, Gutíerrez N, Jørgensen PM, et al. 2012. Evaluación del estado de conservación de los bosques montanos en los Andes tropicales. Ecosistemas 21(1-2):148-166.
- Tufts DM, Revsbech IG, Cheviron ZA, Weber RE, Fago A, Storz JF. 2013. Phenotypic plasticity in blood-oxygen transport in highland and lowland deer mice. The Journal of Experimental Biology 216(Pt 7):1167-1173. https://doi.org/10.1242/jeb.079848
- Vallejos-Garrido P, Pino K, Espinoza-Aravena N, Pari A, Inostroza-Michael O, Toledo-Muñoz M, Castillo-Ravanal B, Romero-Alarcón V, Hernández CE, Palma RE, et al. 2023. The importance of the Andes in the evolutionary radiation of Sigmodontinae (Rodentia, Cricetidae), the most diverse group of mammals in the Neotropics. Scientific Reports 13(1):2207. https://doi.org/10.1038/s41598-023-28497-0
- Van Sant MJ, Oufiero CE, Muñoz-Garcia A, Hammond KA, Williams JB. 2012. A phylogenetic approach to total evaporative water loss in mammals. Physiological and Biochemical Zoology 85(5):526-532. https://doi.org/10.1086/667579
- Van Valkenburgh B, Curtis A, Samuels JX, Bird D, Fulkerson B, Meachen-Samuels J, Slater GJ. 2011. Aquatic adaptations in the nose of carnivorans: evidence from the turbinates. Journal of Anatomy 218(3):298-310. https://doi.org/10.1111/j.1469-7580.2010.01329.x
- Van Valkenburgh B, Pang B, Bird D, Curtis A, Yee K, Wysocki C, Craven BA. 2014. Respiratory and olfactory turbinals in feliform and caniform carnivorans: the influence of snout length. The Anatomical Record 297(11):2065-2079. https://doi.org/10.1002/ar.23026
- Van Valkenburgh BV, Theodor J, Friscia A, Pollack A, Rowe T. 2004. Respiratory turbinates of canids and felids: a quantitative comparison.

- Journal of Zoology 264(3):281-293. https://doi.org/10.1017/S095283 6904005771
- Voss RS. 1988. Systematics and ecology of ichthyomyine rodents (Muroidea): patterns of morphological evolution in a small adaptive radiation. Bulletin of the American Museum of Natural History 188(2):259-493.
- Voss RS. 2003. A new species of Thomasomys (Rodentia: Muridae) from eastern Ecuador, with remarks on mammalian diversity and biogeography in the Cordillera Oriental. American Museum Novitates 3421:1-47.
- Warton D, Duursma R, Falster D, Taskinen S. 2018. smatr: (Standardised) Major Axis estimation and testing routines. https://cran.r-project. org/web/packages/smatr/index.html
- Warton DI, Wright IJ, Falster DS, Westoby M. 2006. Bivariate line-fitting methods for allometry. Biological Reviews 81(2):259-291. https://doi. org/10.1017/S1464793106007007
- Weaver LN, Grossnickle DM. 2020. Functional diversity of small-mammal postcrania is linked to both substrate preference and body size. Current Zoology 66(5):539-553. https://doi.org/10.1093/cz/zoaa057
- Weksler M, Bonvicino CR. 2015. Genus Oligoryzomys Bangs, 1900. In: Mammals of South america. Volume 2, Rodents. Chicago (IL, USA): The University of Chicago Press; p. 417-436.
- Wickham H. 2020. reshape2: Flexibly Reshape Data: A Reboot of the Reshape Package., version 1.4.4. https://cran.r-project.org/web/packages/reshape2/index.html
- Wickham H, Chang W, Henry L, Pedersen TL, Takahashi K, Wilke C, Woo K, Yutani H, Dunnington D, Posit PBC. 2023a. ggplot2: Create elegant data visualisations using the grammar of graphics. https:// cran.r-project.org/web/packages/ggplot2/index.html
- Wickham H, François R, Henry L, Müller K, Vaughan D, Posit Software, PBC. 2023b. dplyr: A grammar of data manipulation. https:// cran.r-project.org/web/packages/dplyr/index.html
- Wickham H, Hester J, Chang W, Bryan J, RStudio. 2022. devtools: Tools to Make Developing R Packages Easier. https://cran.r-project.org/web/ packages/devtools/index.html
- Withers P, Cooper CE, Maloney SK, Bozinovic F, Cruz-Neto AP. 2016a. Physiological characteristics of mammals. In: Ecological and environmental physiology of mammals. Oxford (UK): Oxford Academic; p. 146-289.
- Withers P, Cooper CE, Maloney SK, Bozinovic F, Cruz-Neto AP. 2016b. Physiological adaptations to extreme environments. In: Ecological and environmental physiology of mammals. Oxford (UK): Oxford Academic; p. 290-392.
- Wright KR, Zegarra AV. 2000. Machu Picchu: a civil engineering marvel. Reston (VA, USA): American Society of Civil Engineers
- Xi J, Si XA, Malvè M. 2023. Nasal anatomy and sniffing in respiration and olfaction of wild and domestic animals. Frontiers in Veterinary Science 10:1172140. https://doi.org/10.3389/fvets.2023.1172140
- Xie Y, Cheng J, Tan X, Allaire JJ, Girlich M, Ellis GF, Rauh J, S, Limited Reavis B, Gersen L, 2024. DT: A Wrapper of the JavaScript Library "DataTables." https://cran.r-project.org/web/packages/DT/index.html., et al.
- Yohai VJ. 1987. High breakdown-point and high efficiency robust estimates for regression. The Annals of Statistics 15(2):642-656. https:// doi.org/10.1214/aos/1176350366
- Young KR, León B. 1999. Peru's humid Eastern montane forests: an overview of their physical settings, biological diversity, human use and settlement, and conservation needs. Report number DIVA, Technical Report 5. Centre for Research on Cultural and Biological Diversity of Andean Rainforests (DIVA), Denmark. p. 97.
- Yuk J, Akash MMH, Chakraborty A, Basu S, Chamorro LP, Jung S. 2023. Morphology of pig nasal structure and modulation of airflow and basic thermal conditioning. Integrative and Comparative Biology 63(2):304-314. https://doi.org/10.1093/icb/icad005

# Appendix I

List of collection localities and specimens of Thomasomys spp. analyzed in this study. Abbreviations: MUSM, Museo de Historia Natural de la Universidad Nacional Mayor de San Marcos (Lima); FMNH, Field Museum of Natural History (Chicago); and MEPN, Museo de Historia Natural "Gustavo Orcés V." de la Escuela Politécnica Nacional (Quito). Sex: f, female: m. male.

Thomasomys antoniobracki (n=2): PERU: Piura, Huancabamba, El Carmen de la Frontera, Minera Majaz, Campamento Alto Parramata, -4.894 -79.368, 2630 m (2 m: MUSM 23754, 23755).

Thomasomys aureus (n=1): ECUADOR: Bolivar, Cruz de Lizo, Tatahuazo river, -1.72 -79, 2,600 m (1 f: MEPN 6144).

Thomasomys aff. aureus (n=2): PERU: Junín, Tarma, Huasahuasi, San Pedro de Churco, -11.030 -75.543, 3,217 m (2 m: MUSM 52859, 52860).

Thomasomys aff. caudivarius (n=3): PERU: Cajamarca, San Ignacio, Tabaconas, Piedra Cueva in Cerro Coyona (Tabaconas-Namballe National Sanctuary), -5.268 -79.270, 3,290 m (1 m: MUSM 46711). Piura, Huancabamba, El Carmen de la Frontera, Minera Majaz, Campamento Alto Parramata, -4.90 -79.37, 2,762 m (2 f: MUSM 23562, 23750).

Thomasomys daphne (n=3): PERU: Cusco, Paucartambo, Kosñipata, La Esperanza, -13.178 -71.605, 2,880 m (2 f: MUSM 20014, 20017; 1 m FMNH 175229).

Thomasomys cf. dispar (n=2): COLOMBIA: Huila, San Agustin, San Antonio, 1.948 -76.500, 2,200 m (1 f: FMNH 72397, 1 ?: FMNH 72400)

Thomasomys incanus (n=2): PERU: Pasco, Oxapampa, Oxapampa, San Alberto, -10.531 -75.350, 2,788 m (1 m: MUSM 46187). Junín, Tarma, Huasahuasi, San Pedro de Churco, -11.030 -75.552, 3,309 m (1 m: MUSM 52873).

Thomasomys aff. incanus (n=2): PERU: San Martín, Mariscal Cáceres, Huicungo, Parque Nacional Río Abiseo, La Playa, –7.645 –77.48, 2,650 m (2 m: MUSM 7985, 8002).

Thomasomys ischyrus (n=3): PERU: Huánuco, Huánuco, Chinchao, Caserío San Pedro de Carpish, -9.72418 -76.0994, 2757 m (1 f: MUSM 18346; 1m: MUSM 18347); Huánuco, Pachitea, Chaglla, Palmapampa, -9.88667 -75.88944, 2,900 m (1 f: MUSM 17848).

Thomasomys kalinowskii (n=2): PERU: Huánuco, Huánuco, Chinchao, Caserío San Pedro de Carpish, -9.724 -76.099, 2,757 m (1 m: 18374; 1f: MUSM 18381).

Thomasomys aff. kalinowskii (n = 1): PERU: Pasco, Oxapampa, Oxapampa, San Alberto, 7 Km al este de Oxapampa, límite este del P. N. Yanachaga Chemillén, -10.55 -75.4, 2,200 m (1 m: MUSM 14993).

Thomasomys notatus (n=2): PERU: Cusco, Paucartambo, Kosñipata, Suecia, Km 138.5 Carretera Shintuya, -13.100 -71.567, 1,900 m (1 f: MUSM 17021), -13.101 -71.569, 1,920 m (1 f: FMNH 170690).

Thomasomys pagaibambensis (n=1): PERU: Cajamarca, Chota, Querocoto, Agua de la Montaña, -6.371 -79.153, 2,946 (1 m: MUSM 39737).

Thomasomys cf. pyrrhonotus (n=2): PERU: Piura, Huancabamba, El Carmen de la Frontera, Habas Pite, -5.091 -79.344, 2,117 m (1 m: MUSM 55555); Piura, Huancabamba, El Carmen de la Frontera, Machete, -5.096 -79.347, 2,169 m (1 m: MUSM 55553).

Thomasomys taczanowskii (n=10): PERU: Cajamarca, San Miguel, La Florida, San Miguel, La Florida, Agua Azul, -6.885 -79.075, 1,500 m (2 f: MUSM 15066, 15067); Cajamarca, Chota, Querocoto, Peña Brava, -6.354 -79.140, 2,265 m (1 f: MUSM 39741); Cajamarca, Chota, Querocoto, Agua de la Montaña, -6.371 -79.153, 2,933 m (2 m: MUSM 39735, 39738). Lambayeque, Ferreñafe, Uyurpampa, -6.220 -79.362, 2,827 m (1f: MUSM 21802). Piura, Huancabamba, El Carmen de la Frontera, Habas Pite, -5.091 -79.344, 2,117 m (3 m: MUSM 55562, 55567, 55558); Piura, Huancabamba, El Carmen de la Frontera, Machete, -5.096 -79.346, 2,169 m (1 m: MUSM 55583).

Thomasomys sp. 1 sensu Pacheco (2003) (n=3): PERU: Cusco, Paucartambo, Kosñipata, Morro Leguía, carretera Paucartambo-Pillcopata, Km 135, -13.197 -71.5767, 2,250 m (1 m: MUSM 9349); Cusco, Paucartambo, Kosñipata, Pillahuata, -13.162 -71.620, 2,460 m (1 m: MUSM 19581); Cusco, Quispicanchi, Marcapata, Amacho, -13.575 -70.926, 2,750 m (1 m: FMNH 75588).

Thomasomys sp. 6 sensu Pacheco (2003) (n=1): PERU: Pasco, Oxapampa, Huancabamba, Santa Bárbara -10.339 -75.642, 3,368 (1 f: MUSM 46249).

Thomasomys sp. 9 sensu Pacheco (2003) (n=1): PERU: Cusco, Paucartambo, Kosñipata, La Esperanza, -13.178 -71.605, 2,880 m (1 m: MUSM 20023).

Thomasomys sp. 10 sensu Pacheco (2003) (n=2): PERU: Piura, Huancabamba, El Carmen de la Frontera, Minera Majaz, Campamento Alto Parramata, -4.894 -79.368, 2,630 m (1 f: MUSM 23763); Piura, Huancabamba, El Carmen de la Frontera, Minera Majaz, Campamento Alto Parramata, -4.901 -79.372, 2,780 m (1 m: MUSM 23764).

# Appendix II

#### Morphological description and variation of the turbinal bones.

The genus Thomasomys presents consistent organized and structurally complex turbinals, with clear distinction between respiratory turbinals (nasoturbinal and maxilloturbinal) and olfactory turbinals (semicircular lamina, frontoturbinal 1, frontoturbinal 2, ethmoturbinal I, interturbinal, ethmoturbinal II, and ethmoturbinal III; Figs. 1 and 2). Despite this, notable interspecific variation has been noticed in aspects like lamellar branching, scroll orientation, and relative robustness. We provide a qualitative description of turbinals, including some variations among species.

The nasoturbinal, in coronal view, has 1 root and 2 lamellae: the first, shorter lamella is lateral and located closer to the nasal bone, exhibiting variations such as simple (e.g. T. antoniobracki, T. daphne, T. taczanowskii), or branching (e.g., T. ischyrus, T. pagaibambensis). The second, longer lamella is medial and branches and scrolls angularly (clockwise on the right nasoturbinal and counterclockwise on the left nasoturbinal). Typically, when the scroll is a complete turn or less, it is like a square (e.g., T. antoniobracki); when it is 1 or 1.5 turns, it is triangular-shaped or square-shaped (e.g., T. aff. kalinowskii, T. cf pyrrhonotus). Along the nasoturbinal, the midsection in lateral view is notably more robust in some species, such as those of the Incanus group and larger species of the Cinereus group (Fig. 2; Supplementary Data SD5 and SD6). However, in T. taczanowskii or T. daphne, the robustness of the entire nasoturbinal remains relatively uniform (Fig. 2; Supplementary Data SD5). In addition, the posterior part of the nasoturbinal slightly overlaps with the anterior section of the ethmoturbinal I, with the degree of overlap varying between species, being more conspicuous in some species such as T. ischyrus, T. kalinowskii, and T. sp. 6; and less pronounced in others like T. notatus or T. aureus (Fig. 1; Fig. 2).

The maxilloturbinal, attached to the maxillary bone and located under the nasoturbinal in coronal view, exhibits considerable variation along its length (Fig. 2; Supplementary Data SD5). The maxilloturbinal has 1 or 2 roots and 2 major lamellae: the first, longer lamella ascends and comes closer to the nasoturbinal, scrolling dorsally and angularly for one complete turn (clockwise on the left maxilloturbinal and counterclockwise on the right maxilloturbinal). This lamella typically features 1 or 2 small branches, but occasionally it is simple (as seen in T. daphne and T. aff. aureus). The second lamella is shorter, ventrally angular scrolled, and sometimes branches in the middle into 2 or 3 slightly straight sub-lamellae, 1 longer than the others. Along the maxilloturbinal, the robustness can also remain relatively constant from the anterior to the posterior part in sagittal view, but the posterior portion always tapers to a sharp point, being unattached to the maxillary bone (Fig. 2; Supplementary Data SD5). The maxilloturbinals are anteriorly placed similarly to the nasoturbinal. Both structures are of similar size and respectively positioned ventrally and dorsally in the rostrum. However, significant exceptions exist (Fig. 2). Notably, in T. cf caudivarius and T. aff. incanus the nasoturbinal is more elongated than the maxilloturbinal (Fig. 2; Supplementary Data SD5).

In all species, the semicircular lamina—which is the superiormost olfactory turbinal—displays notable variation in its structure (Fig. 2). In a sagittal view, it is anteroposteriorly elongated and protruded medially in the dorsoventral direction. This protrusion joins the dorsal side of the ethmoturbinal I. The frontoturbinal 1, in coronal view, has 1 root and 2 divergent lamellae, both exhibiting a slight dorsoventral scroll, typically less than 1 full turn. Sometimes, the lamellae closer to the semicircular lamina may feature a single straight small projection, as observed in T. pagaibambensis or T. ischyrus. The frontoturbinal 2, in coronal view, is typically composed of 1 lamella that is slightly scrolled dorsoventrally, as seen in species like T. oreas. However, in less common cases, it consists of 2 divergent lamellae—1 positioned dorsally and the other ventrally in relation to their orientation within the nasal cavity. Both lamellae are slightly scrolled, with the dorsal one being shorter and the ventral one being longer, as seen in T. kalinowskii. Usually, frontoturbinal 1 is as long as frontoturbinal 2, except for T. cf. dispar and T. daphne (Fig. 2). The ethmoturbinal I, being the largest olfactory turbinal, exhibits a prominent projection toward the rostral side. Its structure in coronal view is characterized by a delicate, very complex arrangement of thin scrolls and plates. The ethmoturbinal I protrudes medially in the dorsoventral direction, which is notably wide in T. daphne and T. antoniobracki, and its anterior part extends to the posterodorsal region of the nasoturbinal. The interturbinal, located between the ethmoturbinal I and ethmoturbinal II—seen in coronal view—consists of a single lamella that is slightly ventrally scrolled, typically less than 1 full turn. It is the simplest turbinal, and its structure remains relatively consistent with minimal variation along its length in sagittal view. The ethmoturbinal II formed 1 root and 2 lamellae, one lamella dorsal and straight and the other lamella ventral and slightly scrolled, less than 1 full turn. The ethmoturbinal III, seen in coronal view, formed one slightly scrolled lamella, which sometimes has a small projection in the middle before scrolling, as observed in species of the Incanus group. In most Thomasomys species, the frontoturbinals, interturbinals, and ethmoturbinals are notably elongated in sagittal view, except for smaller species like T. daphne and T. taczanowskii where these structures are shorter (Fig. 2).

Variation in turbinal bones is evident not only in the complexity of branching of individual lamellae, but also in how these structures occupy the nasal cavity. Species with larger and more complex turbinals, as evidenced by our quantitative analyses such as those from the Incanus group, can be easily identified because turbinals fill almost the entire nasal cavity. While in species with smaller and less complex turbinals, such as the small-sized species T. taczanowskii or Thomasomys sp. 9, their nasal cavity is not filled with turbinals (Fig. 2).